A mining research contract report

DECEMBER 1983

FIELD TEST OF A POST-DISASTER COMMUNICATION SYSTEM

Contract J0123030

University of Michigan

Cooley Electronics Laboratory

BUREAU OF MINES
UNITED STATES DEPARTMENT OF THE INTERIOR

The views and conclusions contained in this document are those of the authors and should not be interpreted as necessarily representing the official policies or recommendations of the Interior Department's Bureau of Mines or of the U.S. Government.

50272-101

REPORT DOCUMENTATION PAGE	1. REPORT NO.	2.	3. Recipient's Accession No.

4. Title and Subtitle Field Test of a Post-Disaster Communication System	5. Report Date December 1983 6.
7. Author(s) M. P. Ristenbatt, E. K. Holland-Moritz, K. Metzger	8. Performing Organization Rept. No. 019965-F
9. Performing Organization Name and Address Cooley Electronics Laboratory The University of Michigan Ann Arbor, Michigan 48109	10. Project/Task/Work Unit No. 11. Contract(C) or Grant(G) No. (C) J0123030 (G)
12. Sponsoring Organization Name and Address U. S. Bureau of Mines Pittsburgh Mining & Safety Research Center Pittsburgh, Pennsylavania 15213	13. Type of Report & Period Covered Final 14.
15. Supplementary Notes	

16. Abstract (Limit: 200 words) A new post-disaster signalling system for the Bureau of Mines, using through-the-earth EM propagation, was successfully field-tested in the Lake Lynn test mine. Successful detection at an estimated input SNR of -30dB was accomplished using a coherent integration time of 4.46 minutes.

The transmitted waveform consisted of a repeating pseudonoise maximal length sequence phase modulating a 1950Hz carrier. The receiver used a sliding-window matched filter, optimal for signal known exactly except for phase and starting time, implemented via a special purpose processor. Parallel processing permits adaptive signalling, where the detection (integration) time is determined by the actual input SNR encountered.

This field test demonstrates a trapped miner detection system that is about 36dB more sensitive than a current pulsed system. This increased sensitivity permits some desired combination of increased range, shorter detection time, and reduced transmitter power or antenna-size. The combination of pulse-compression-type-signal, coherent integration, parallel-processing, and output peak-detection algorithms permit implemention of an ultra-reliable detection system. The same combination is compatible with digital Pulse Position Modulation and Emitter position location strategies.

17. Document Analysis a. Descriptors

Mine Communications
Trapped Miner Communication
Adaptive Communications
Spread Spectrum
Feedback Communications
Coherent Detection
Emergency Communications
Digital Communications
Through-the-Earth-Propagation
High TW Signaling
Matched Filtering
Maximal Binary Sequences
Signal Processing

c. COSATI Field/Group

18. Availability Statement	19. Security Class (This Report) Unclassified	21. No. of Pages 51
	20. Security Class (This Page) Unclassified	22. Price

(See ANSI-Z39.18) See Instructions on Reverse OPTIONAL FORM 272 (4-77) (Formerly NTIS-35) Department of Commerce

FOREWORD

This report was prepared by The University of Michigan, Cooley Electronics Laboratory, Ann Arbor, Michigan under USBM Contract number J0123030. The contract was initiated under the Coal Mine Health and Safety Research Program. It was administered under the technical direction of the Pittsburgh Mining and Safety Research Center with Steven Shope as Technical Project Officer. Doyne W. Teets was the contract administrator for the Bureau of Mines. This report is a summary of the work recently completed as a part of this contract during the period June 1982 to September 1983. The draft report was submitted by the authors in December 1983.

Steven Shope was responsible for all the physical arrangements for the data taking, and supervised the analog recording at the surface. He operated the transmitter within the mine, and provided FFT-type analysis results of both transmission and surface-received signals.

The authors wish to acknowledge the technical discussions with T. G. Birdsall of CEL's Signal Processing Group, and acknowledge the use of his (ONR sponsored) signal processing equipment and expertise. The availability of these items, at no cost to the Bureau of Mines, made it possible to accomplish significant tests with a minimum budget.

TABLE OF CONTENTS

FIELD TEST OF A POST DISASTER COMMUNICATION SYSTEM

by

M. P. Ristenbatt, E. K. Holland-Moritz and K. Metzger

1. Introduction

The objective of this effort was to document the field performance of a post disaster mine signalling system that recently has been demonstrated in the laboratory (Ref. 1, 2). The three major objectives of our effort were: 1) prepare transmitters by designing and adding a new signal generator to an existing Bureau of Mines transmitter; 2) cooperate with the Bureau of Mines in obtaining recorded data during field tests; and 3) process and analyze the tape recorded data from the field test.

2. Background

The Bureau of Mines currently has a signalling system which is intended to permit a trapped miner to transmit a periodic signal to the surface, or to an interior receiver, using through-the-earth electro-magnetic wave propagation. The transmitted signal is a low audio frequency pulse with a duration of 0.1 second which repeats every second. The frequency of the tone is selected to fall between the harmonics of 60 Hz, which are significant background noise contributors. The receiver picks up the signal on a loop antenna and translates it to 1000 Hz. The signal is narrowband filtered and presented to the operator by earphones and a visual meter indicator. The output of the receiver consists of the noise from the (30 Hz-wide) carrier frequency band translated to 1000 Hz accompanied by possible 1000 Hz signal pulses. Detection in a noisy background depends on a number of successive signal pulses being high enough above the (1000 Hz) background noise so that the operator can recognize the 1 second spacing. In effect, the receiver consists of a "front-end" bandpass-amplifier, in combination with the ear (or eye) plus brain.

After a signal is detected, the operator uses horizontal (walking) displacement, and rotation of the loop to locate nulls in the vertical or horizontal magnetic field of the transmitter. This allows locating a point directly above the transmitter.

In our predecessor laboratory demonstration work (Ref. 2), we verified, using observer tests and theoretical models, that in

Gaussian noise, this system requires an input signal-to-noise ratio (SNR) of about 6 dB for specified detection performance.

A prior study (Ref. 1), showed that signal detection at a much lower SNR would be possible in the Mine Disaster Communication system if; 1) the 1/10 second carrier pulse, repeated each second, were replaced with a continuous carrier phase modulated by a repeating binary pseudo-noise (PN) maximal sequence; and 2) the human operator with earphones were replaced by a digital matched filter for coherent integration of one or more periods of the binary PN signal.

Important aspects of the new system are:

1) coherent integration of the signal "known exactly except for phase and starting time," over time intervals from (say) 17 seconds up to (say) 17 minutes.

2) the PN (maximal-length sequence) signal implements a large time-bandwidth product signal, having an ideal autocorrelation. The transmitted PN signal is a constant amplitude phase-modulated signal. At the same time, the receiver output, after matched filtering, is a pulse occuring at one of 255 possible pulse positions. This provides: (a) a practical way for observing the actual noise background during signalling, at the times between pulses. (b) the ability to receive up to 255 different signals without interference in one 30 Hz bandwidth based on different PN sequence starting times (assuming no oscillator drift). These could be alarms from other miners or signal codes used for communication during rescue operations. (c) a receiver which can be made more resistant to both pulse and CW interference than the present pulse receiver. (d) a continuous transmitted signal which can be measured by a simple receiver for locating nulls, after the signal phase and sequence starting time are determined by an alarm receiver.

3) a parallel receiver processing is used which simultaneously tests for potential alarm signals after integration over 1, 4, 16 and 64 sequence periods. This allows rapid response to strong signals, without the risk of losing alarms under less favorable conditions.

In the immediately preceding work (Ref. 2), we demonstrated in the laboratory successful operation in white Gaussian noise at an input SNR of -34 dB.[1] This performance required coherent

[1]Gaussian noise is the worst case, since it is unpredictable except for its statistical properties. The actual mine noise includes periodic components and pulses which can be suppressed more easily than Gaussian noise.

integration of 17 minutes. This maximum potential decrease of required input SNR by 40 dB, from the 6 dB of the present system to the potential -34 dB of the proposed system, permits some desirable combination of: 1) reducing the transmitter current or antenna magnetic moment; 2) increasing the reliability and/or extending the system range; 3) using a moderate detection time (say 17 seconds), with automatic back-up for less favorable conditions; and 4) increasing the accuracy or reliability of null location in noisy backgrounds.

The PN maximal sequence is a particularly favorable choice of bits for efficient transmission because it has a constant envelope and an ideal pulse autocorrelation function. The output of the PN matched filter for each 255 chip[1] sequence is one signal pulse and 254 other possible pulse positions where noise measurements can be made, or other PN signals received. The constant envelope of the PN signal allows the output pulse power for 16 sequence repetitions to be (16x255)=36 dB higher than the peak pulse power for a TW=1 signal.[2]

Additional improvement in the performance of the PN system is possible if the noise is non-Gaussian. For example, if the noise consists of isolated pulses, only that portion of the pulse power which falls in the PN signal bandwidth appears at the PN output. The same matched filter processing which converts the PN transmitted signal to a pulse output, takes the pulse power in the PN bandwidth and spreads it uniformly over the PN signal integration time. If the PN pulse detection system compares possible pulse positions with the background noise, it only measures an increased continuous background, without pulses, no matter how large the power in the isolated pulse. False alarms due to isolated pulse noise can occur only if there are many large pulses in the PN integration period. When this is the case, the constant envelope of the PN carrier can be exploited by using a limiter ahead of the PN matched filter to limit the peak received input signal amplitude to the (observed in some fashion) amplitude of the PN signal plus background Gaussian noise. This reduces all pulse noise to small pulses. The residual effect of many clipped pulses is both to reduce the signal peak and to increase the effective Gaussian noise background. Nevertheless, a limiter is very effective in a PN system especially when large or unpredictable noise pulses are present.

A limiter is much less effective in a (TW=1) pulse system, because it cannot limit the noise without limiting the peak output pulse to the same level. With PN processing the output

---

[1] A "chip" means one modular part of a total signal; the number of chips essentially means "number of independent samples in the signal," and hence, equals the time-bandwidth (TW) product of the signal (255 here). A simple pulse signal, as in the present system, has a nominal TW product of 1.

[2] In this application, the peak transmitter power is limited both by the miner's battery and by mine safety restrictions.

signal pulse power is increased by a factor equal to the TW product after the limiting.

It may not be obvious, but a very similar suppression of isolated CW interference can occur in a well designed PN system. This type of interference can occur from harmonics of portable power generators operating slightly off 60 Hz frequency, harmonics generated by induction motors, and some types of starting and stopping transients. This exploits the PN-signal nulls at harmonics of 60 Hz (see Fig. 3 of Ref. 2).

From the above, we see that the noise-like PN matched filter is much more efficient in suppressing both the pulse and the CW interference than the matched filters for either pulse or CW signals alone. It simultaneously combines the best features of both, and adds some features of its own. Unless the interference is extremely strong, this may be all the protection which is needed. As will be described, on the second mine test day, the pulse and pulse burst interference was very strong. In this case, a limiter ahead of the PN filter can reduce the noise at the system output as was demonstrated later in our off-line processing results.

After an alarm signal is detected, the PN signal used here is an excellent signal for digital data transmission. Hence, post-detection communication may utilize a real time voice downlink with either a digital data or an off-line digital voice uplink.

3. Equipment Preparation

3.1. PN Encoder

As noted, the University of Michigan Post Disaster Communications System uses a continuous carrier phase modulated by a digital pseudo-noise signal. The transmitter for the field tests was implemented by adding a new signal source to the existing Bureau of Mines pulsed VF transmitter (Circuit A1A2, General Instrument Ref. 3).

As specified by the contract, two of the transmitters available for use in the present system were modified to generate and continuously transmit a 1950 Hz carrier phase modulated by a 255 chip-long maximal sequence, at a chip-rate of 15.23 chips/second.[1] There are 128 carrier cycles in the 65.64 ms-long

[1]The signal spectrum nulls could be centered exactly on the harmonics of 60 Hz by using a 15 Hz chip-rate and 32.5 cycles of carrier per demodulate. This would be compatible with the present receiver algorithms. However, using an integral number of cycles per demodulate may be slightly more efficient in rejecting low frequency noise and A/D offset errors. We chose to use 32 cycles per demodulate, but 32.5 is a viable option.

chip. The resulting signal power spectral density has a $(\frac{\sin x}{x})^2$ envelope with a main lobe width of 30.46 Hz. It lies midway between the 32nd and 33rd harmonics of 60 Hz and has broad nulls at those harmonics.

The choice of a 255-long sequence, made in the original design effort (Ref. 1), considered the background noise to be Gaussian and was based simply on the criteria that we desired a sufficient number of "noise-only" sample values between output peaks (when the signal is present), and the operational consideration of minimum decision-delay time. It was assumed that RF-filtering would suppress any harmonics of 60 Hz adjacent to the carrier. Further experience convinced us that the filtering should be done by the signal processor itself, so that some harmonics of 60 Hz may be present at the processor input.

It may be advantageous, from the signal processor point of view, to consider a sequence-length of 63. It is not yet clear whether this change would decrease the processor gain against the harmonics, but will be studied in the future.

Figure 1 shows the General Instrument circuit diagram (their Figure 2-2, p. 11) from their final report (Ref. 3), along with the PN encoder connection points. A carrier frequency of 1950 Hz was recommended by the Bureau of Mines, based on considerations of both propagation loss and noise behavior. The logic circuit diagram of the PN encoder that was designed is shown in Fig. 2. In the previous laboratory test (Ref. 2), our transmitted signal was a sinusoidal carrier which was digitally generated and digitally phase modulated. The Bureau of Mines transmitters supplied for the present contract requires a binary digital input and supplies a square wave carrier voltage to the transmitter loop antenna. After filtering by both antenna systems and the receiving filters, the received signal carrier is sinusoidal in both cases. An improvement, relative to the prior-effort signal generator, was made in the efficiency of the PN signal generated by the new boards. In our previous contract (Ref. 1), the PN phase modulation of the carrier was 180°. Since there are an odd number of bits in a maximal PN sequence, this actually results in a signal with a reduced value at the carrier relative to the adjacent signal sidebands. In the time domain, the receiver output has an offset (minus-one) between the pulse-compressed auto-correlation peaks. In the new board the phase modulation angle is 172.8°, which eliminates the minus-one offset between peaks, and produces a processed output signal with the ideal zero-referenced autocorrelation function. This technique was developed by Prof. T. G. Birdsall and Dr. Kurt Metzger in connection with their long-standing work in utilizing PN sequence signals for studying the properties of underwater sound propagation, and is thoroughly detailed in Ref. 4.

Coherent integration, in the absence of strong carrier,

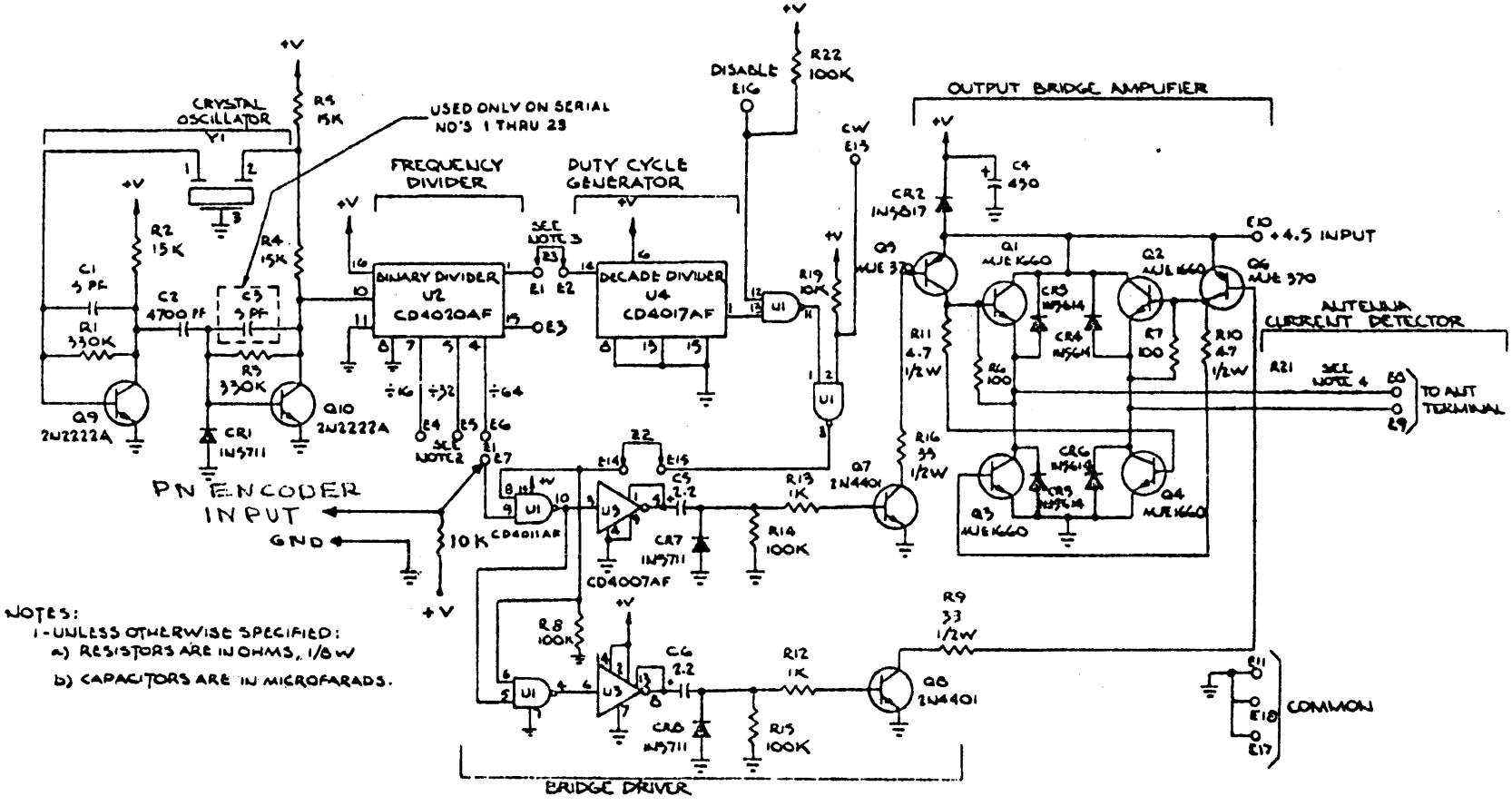

Note: The original circuit had antenna current detector which was not in the units supplied to us.

Figure 1. PN-Encoder to VF Board Connection Diagram

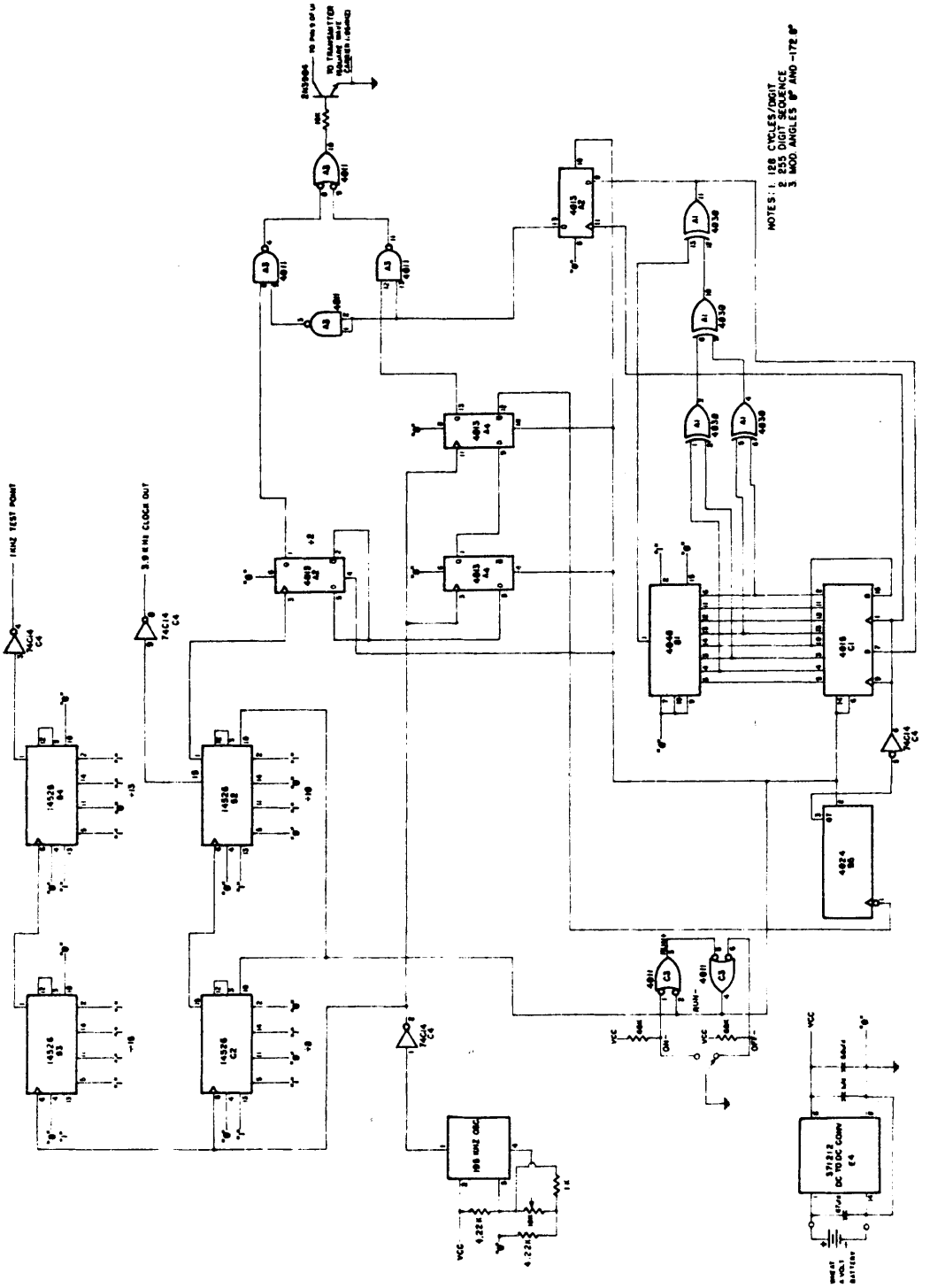

Figure 2. PN Encoder Circuit Diagram

requires clock stability at both transmitter and receiver that is commensurate with the maximum integration time. The basic criterion is that there be substantially less than 180° phase shift, at the carrier frequency, over the total integration time.[1]

If we upper bound the integration time as being in the order of 10 minutes, then the total number of "parts" involved is:

$$(1950 \frac{\text{cycles}}{\text{sec.}}) \times 600 \text{ sec.} = 1.17 \times 10^{6} \text{ total} \qquad (1)$$

If we choose to keep the phase-shift to about 10% of one part in the 10 minutes, then the required stability is:

$$\text{Req. Stability} = \frac{.1}{1.17 \times 10^{6}} = .85 \times 10^{-7} \approx 1 \times 10^{-7} \qquad (2)$$

Thus, a stability of one part in 10^{7} was selected for these test transmitters.

This criterion led to our selecting the Vectron Labs (CO-252B17V) crystal oscillator, which, ground to our custom frequency, cost $410.00. This cost would decrease with volume purchases.

The oscillator module and PN phase modulator are mounted on a circuit board similar to the present transmitter boards as shown in Fig. 3 and in the photograph of Fig. 4. This unit could fit into the present VF transmitter boxes above the existing circuit board. However, since the power transistors on the VF transmitter board are a significant source of heat, we thought it desirable to mount this new board in a separate box, to isolate the crystal thermally. This may not be necessary in practice, but appeared to be a sensible precaution at this field-testing phase. (One of our secondary objectives was to exploit the natural opportunity to determine the source of any limitations). This arrangement allowed us to distinguish, in the laboratory, between residual frequency drift due to temperature variations and frequency drift due to supply voltage variations.

3.2. Signal Processing

The general concept for the signal processing was described in the report for the predecessor effort (Ref. 1), and will only

---

[1] The long term stability requirement for the transmitter can be relaxed, but only at the cost of increased receiver complexity. More complicated algorithms for underwater acoustic signals can detect doppler shifted PN sequences with unknown frequency shifts. The phase of the received signal as a function of time was in fact displayed as part of each of the present tests. However, no correction for the phase errors was included in the processing algorithm.

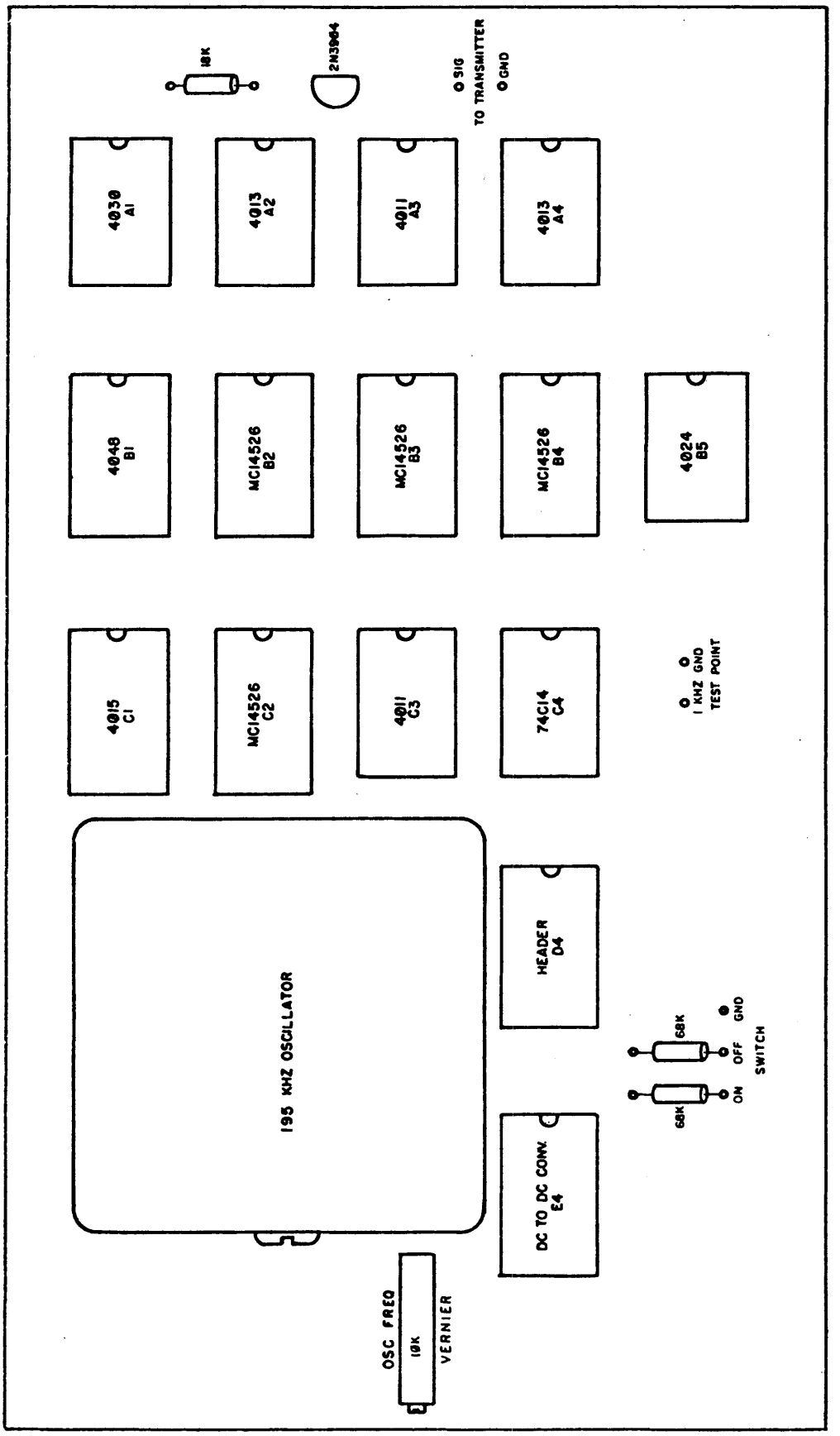

Figure 3. PN-Encoder Circuit Board Arrangement

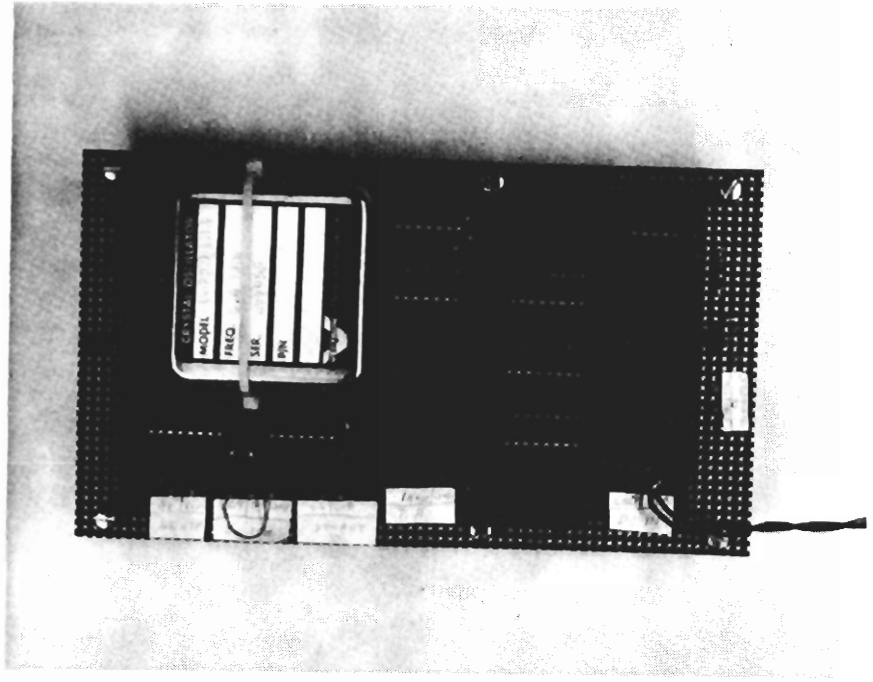

Figure 4. PN-Encoder Circuit Board

be synopsized here. The essential idea is to first demodulate the signal using the traditional complex demodulator, to generate 4 inphase and 4 quadrature demodulates per sequence chip (a sequence bit is one "chip" of the entire integrated signal). The digital matched filter processes the inphase and the quadrature components separately in increments of 1/4 sequence chip. The matched filter outputs for successive periods are added coherently for various integrating times: 1 sequence-length (16.74 seconds); 4 sequence-lengths (66.954 seconds); 16 sequence-lengths (4.46 minutes); and 64 sequence-lengths (17.854 minutes). For each integration time, the 4 demodulates per chip are averaged by a sliding window. The inphase and quadrature components are then combined as the sum of squares. Processing the received signal simultaneously with different periods of coherent integration permits a receiver to "alarm" at the shortest time, after onset, commensurate with the received SNR. With the parameters chosen here, an alarm could occur at 17 seconds after onset if the SNR is adequate, and at one of the longer times for lower received SNR's.

The signal processing software and hardware used to process and display the PN signals were small special purpose computers programmed to demodulate the signal and then to operate as matched filters either for the sequence itself, or for a periodic signal consisting of 4, 16 or 64 repetitions of the PN sequence. The output of the digital matched filters is a "time compressed" pulse with a (two-sided) duration of twice the chip length occurring once every 16.74 seconds.

The actual equipment used for processing and display was designed and constructed by the CEL Signal Processing Group mentioned before (T. G. Birdsall and K. Metzger). The equipment was designed and developed for processing acoustic signals in Oceanography. It was reprogrammed to match our signal and display parameters.

Figure 5a repeats (from Ref. 1) the general classical concept for matched filtering to a "signal known except for phase and starting time," for the particular signal parameters used here. In effect, the entire PN signal, over 1, 4, 16 or 64 sequence epochs, is known except for the uncertain turn-on plus propagation-delay time. The proper receiver, in terms of classical communication principles, would be called "a complex demodulator for a large time-bandwidth-product signal."

The signal is first band limited in a 1/10 octave filter. As indicated in Fig. 5a, the signal is then sampled and A/D converted at four times the carrier frequency (4 x 1950 = 7800 samples per second). An inphase demodulate, corresponding to multiplying by the $\cos 2\pi(1950)t$, is obtained by forming the sum of the first samples of each cycle for 32 consecutive cycles, then forming the sum of the 3rd samples for the same 32 cycles, and subtracting the two sums. Similarly, a quadrature demodulate

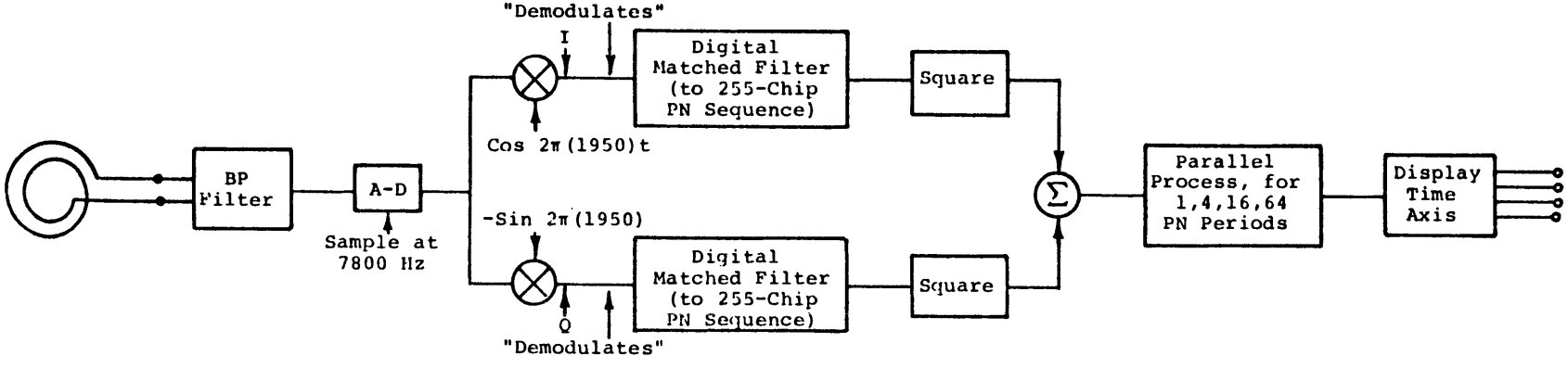

(a) Classical Concept of Complex Demodulator and Parallel Processing

Figure 5. Block Diagram of Signal Processing Arrangements

is derived, corresponding to multiplying by $-\sin 2\pi(1950)t$, by forming the sum of the 2nd samples for 32 cycles, then forming the sum of the 4th samples for 32 cycles, and subtracting the two sums. The inphase and quadrature demodulates are time-interleaved, and appear sequentially at the output as 8 real numbers per chip.

During the predecessor-effort laboratory demonstration, the complex demodulation processing and recording the demodulates on digital tape was done in a CEL computer. The matched-filter integrating was done off-line on the University of Michigan time-sharing MTS AMDAHL computer. For this present effort, we were able to exploit further equipment development by Messrs. Birdsall and Metzger. In particular, a new portable processor (called DM1200) became available. The DM1200 is a special processor (17" x 17 1/2" x8 1/2") designed and built at CEL, using standard mother-board construction, with a 24K byte memory. For off-line processing, the DM1200 forms the complex demodulates and performs the matched filter operations.

As indicated in Fig. 5b, the DM1200 was used twice in the off-line processing. The MTDEMOD program was used first, to form demodulates which are stored on digital reel-to-reel tape. Then, using a tape playback for these demodulates, the DM1200 is used again with an MTXC program which cross-correlates the demodulates with the PN sequence reference. The output is an uncombined 4 chips per bit, and is essentially the matched filter or correlated output for a single PN sequence epoch. This is again stored on a digital reel-to-reel tape. In effect, the correlation slides the reference-sequence along the data samples in increments of 1/4 chip resolution. This off-line processing permits detailed examination of the data.

A final step at the time-shared U-M Computing Center first coherently combines the 4 chips per bit, and then coherently averages the results over 1, 4, 16 and 64 PN sequence epochs. The filtered inphase and quadrature samples for each sliding window position are then squared and added for the final output. A print-out program permits tallying the entire sequence of output numbers, for each instant, which provides quantitative data for the peak values and the intervening noise-only values (see Appendix A).

Perhaps the most important role of the DM1200 was its use of another program for real-time processing (see Fig. 5c). This permitted us to process the field data in real time to find the operating threshold for the system. As noted in Fig. 5c, the real-time processing used the SCMP program in the DM1200 processor, which produced a graphical display on a CRT which could be copied on a printer.[1]

[1] At the time of signal processing, this program did not provide numerical data for the output SNR for each trace. These values were later added to the other data printed under each trace.

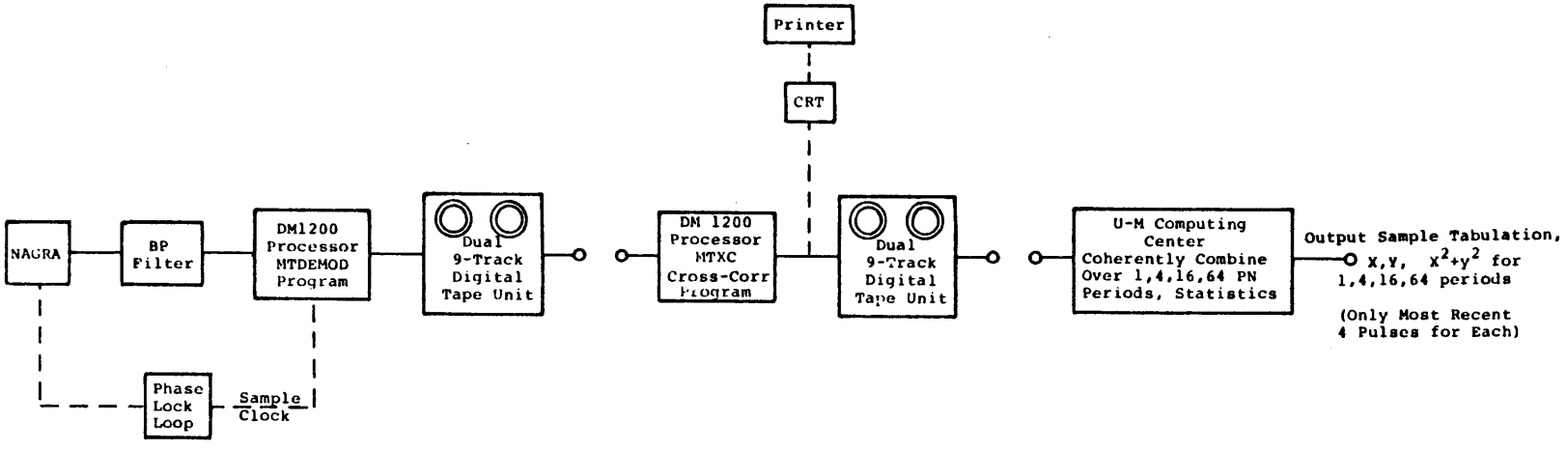

(b) Off-Line Processing Used for Numerical Printout of Data

Figure 5. Continued. Block Diagram of Signal Processing Arrangements

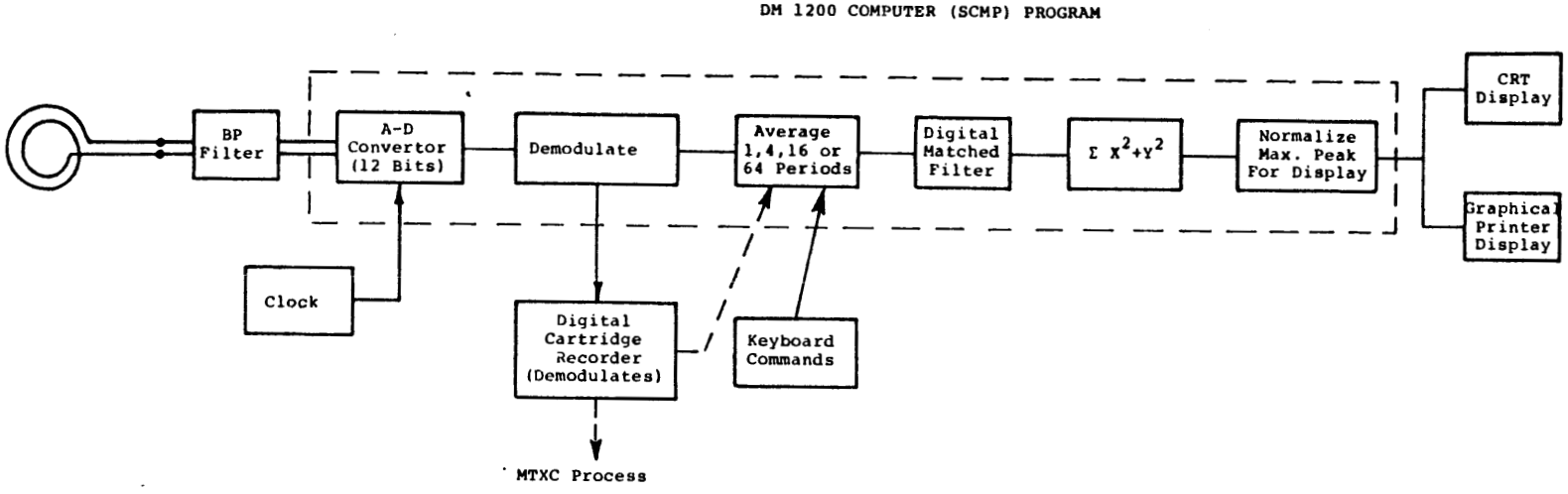

(c) Real-Time Processing Permitting On-Line Monitoring During Field Tests

Figure 5. Continued. Block Diagram of Signal Processing Arrangements

A digital cartridge tape recorder was also borrowed (from the underwater acoustics project) and used for on-line recording of the SCMP demodulates. This served as a back-up to the field-test analog tapes, and did not require a timing track and recorder calibration (a 7800 Hz timing track was recorded for the analog tapes, and tape calibration was required).

Both the off-line and the real-time processing arrangements were first tested in our laboratory in Gaussian noise; then between different floors in the background noise of our laboratory, and finally in mine-to-surface transmissions in the field tests.

4. Test Configuration

4.1. Physical Site and Arrangement

The field tests occurred on Wednesday, June 29 and Thursday, June 30, 1983, at the Bureau of Mines Lake Lynn test-mine. This limestone mine which is near Uniontown, Pennsylvania, has an overburden of 100 meters at the test-position. The arrangement for the facility, the general test plan and configuration, and supervision of the data taking was the responsibility of the Bureau of Mines (handled by Project Officer Steven Shope). During the tests, S. Shope operated the transmitter and made all associated measurements. The analog tape recorder on the surface was operated by Bureau of Mines personnel (Carl Gonoe). The real-time processing equipment and digital recording apparatus was operated by Dr. K. Metzger of CEL.

Figure 6 shows the general equipment arrangement used in the field tests. The underground loop antenna consisted of one turn of 300 feet (91.4 m) of #12 copper wire deployed in a rectangle resulting in a loop area of 2144 square feet (200 square meters). The current flowing in the loop was measured by the AC voltage drop across a small resistor placed in series with the loop on a Nagra tape recorder. The RMS current at the center frequency any time during the test could be obtained from the output of FFT computer, either directly at the mine or from the tape playback.

4.2. Field-Test Recording and Monitoring

The major data taking arrangements are also shown in Fig. 6. A Bureau of Mines (Collins) loop antenna fed a (U-M) pre-amp (Gain=666), followed by a one-tenth octave (General Radio) filter centered at 1950 Hz. The input resistance of the pre-amp was about 200 kΩ , and a capacitor was placed across the loop terminals to make the loaded antenna resonate at 1950 Hz. Also, some additional electrostatic shielding of the loop was accomplished by wrapping the loop with aluminum tape. This reduced electrical noise pick-up in our noisy laboratory, and may have been helpful in the field.

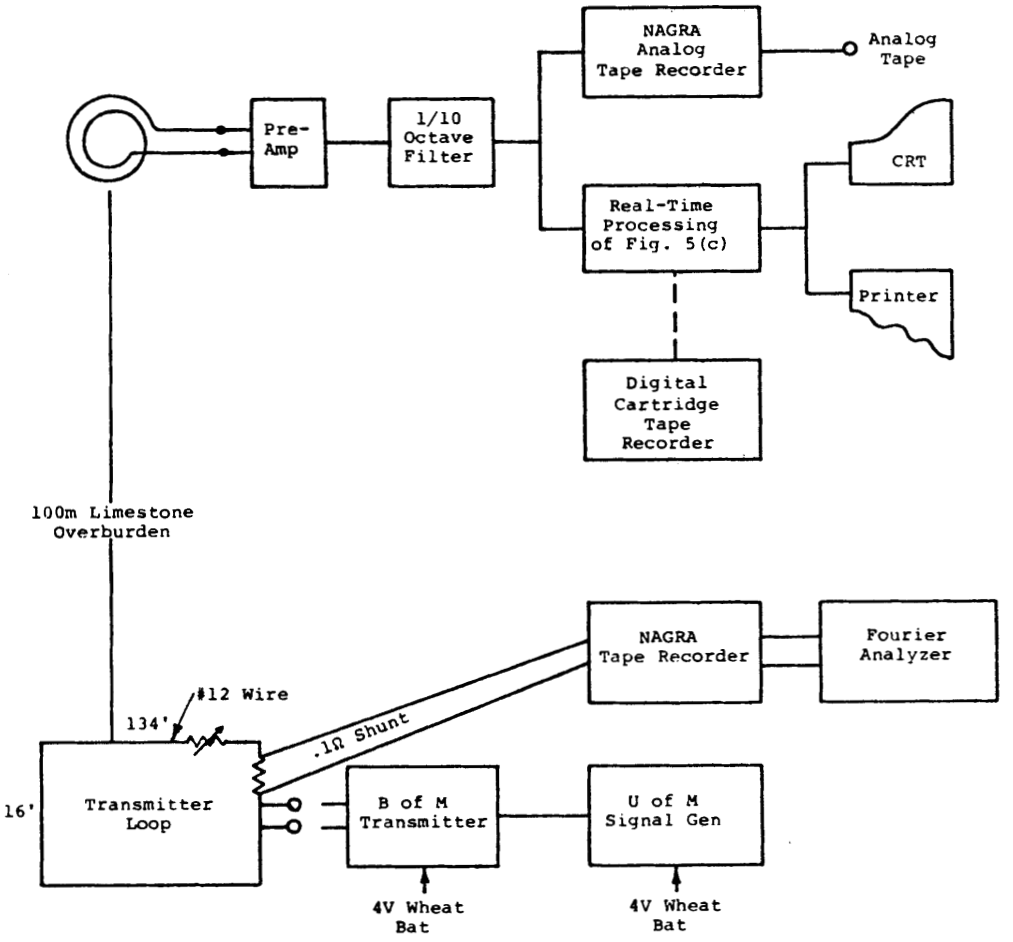

Figure 6. General Equipment Arrangement for Field Tests

Two major data-taking thrusts occurred during the field tests: 1) analog recording, for later processing, of the received signal on channel 1 of an analog-reel tape, with a 7800 Hz timing signal derived from a rubidium frequency standard recorded on a second channel, (this taping was done by the Bureau of Mines); 2) real-time processing and display for one-integration time only (16 sequence periods = 4.46 minutes), plus digital-cartridge recording of the unaveraged demodulates for later processing. While the original field-test plan envisaged only the analog recording, we found we could use the DM1200 to process the averaged signal in real time in the field to determine the threshold signal level, and at the same time provide a digital back-up for the analog tape recordings.

The analog recording at the receiver site was done using a NAGRA IV-ST tape recorder supplied and operated by the Bureau of Mines. As already noted in Sec. 3.2, real-time processing averaged over 16 sequences was done at the site using the (CEL) DM1200, which calculated the demodulates and recorded the demodulates in real-time onto the digital cartridge tape. It also added the 16 periods and performed the matched filter operations on each 16 period signal average. To avoid overloading the displays, the highest peak in each display line was normalized to unity.

4.3. Test Series

The data was taken on two contiguous days, Wednesday, June 29, and Thursday, June 30, 1983. Wednesday morning was spent driving to the receiver site in a wooded area over the transmitter location. The receiving and recording equipment was set up in the back of a pickup truck and operated on AC power supplied by a gasoline engine-driven alternator.

We chose to run each test for a period corresponding to the length of the analog tape reels. This permitted only two periods of the longest (17 minute) multiple integration times. The five data runs that will be described are listed in Table 1.

On Wednesday, the noise background was relatively stable, consisting mainly of harmonic noise plus Gaussian. For the Thursday tests, the noise from harmonics of 60 Hz was the same as the previous day, but the noise from short random pulses and large noise bursts was at least 12 db higher than the previous day. We assume that the increase in short random pulses was due to atmospherics from a wide front of thunderstorms passing through the area. The large noise bursts appeared random to us. However, in playing back the tapes, we found that they consist of main noise bursts occurring every 45 seconds, each followed about 6 seconds later by a second noise burst, usually lower in amplitude but longer in duration. Figure 10 (later) illustrates both the increased small pulse activity and the very large pulse pairs which were present on Thursday.

TABLE 1. DESCRIPTION OF FIELD TEST DATA

Test Name	Time	Duration	Antenna Current (mA)	Estimated Input SNR (dB)			Rationale for Signal Level	Comments
				Impulse Noise Excluded		Includes Impulse Noise		
				22 Hz Measurements	Theoretical Predictions	Based on Output Peak-To-Noise-Only		
A	2:00pm Wed.	35 min.	88.25	20.4	23.8	23.4	Wanted level high enough to permit on-site equipment check-out, and later detailed diagnostics (such as phase behavior)	Normal background noise; drop-outs occurred on time reference due to poor quality tape
C	3:00pm Wed.	35 min.	10.37	2.14	5.6	9.4	Wanted significant (20 dB) reduction from Test A	" "
E	12:25pm Th	35 min.	0.25	-30.8	-27.2	-42.627	Wanted repeat of Wednesday probe for threshold; no in-field detection	Observed in field that noise increased over Wednesday; large bursts occurred
P	2:09pm Th	35 min.	0.68	-19.9	-18.4	-36.6	Increase 6 dB, looking for field detection. None found.	" "
Q	3:05pm Th	35 min.	1.28	-11.7	-13.3	-24.227	Increase another 6 dB, looking for field detection. Signal was detected.	" "

5. Specific Signal Processing Methods Used

Figure 7 shows how the analog and digital playbacks were handled, using the SCMP program for matched filter averaging and time display outputs. For analog, the input to the DM1200 computer was the output of the 1/10 octave filter and is the same signal as was recorded on the NAGRA recorder. The 7800 Hz sample clock signal is also the same as that recorded on the NAGRA. The signal input was sampled and converted at the 7800 Hz clock rate. The output of the demodulates consists of 4 inphase (x) demodulates and 4 quadrature (y) demodulates per sequence bit. The x and y sample outputs are interleaved. The keyboard controls whether these demodulates are recorded on the digital cartridge recorder, and whether averaging over 4, 16 or 64 sequence periods was done before further processing. All of these operations were done in real time by the DM1200 computer using some handwired logic boards as well as the SCMP program.

The rest of the present SCMP program runs a little slower. For averages over 4 periods or more, it can process the averaged data in real time. Without averaging, it accepts new samples for on-line processing only when it is finished with the previous set.

Notice that the signal to the display is normalized so that the largest peak, whether signal or noise, is a full scale deflection. The CRT displays up to 8 output pulse traces before erasing and starting over. Each output trace is identified by a trace number and the x coordinate position of the maximum peak. The phase of the received signal at some specified x coordinate can also be printed on the display. This can be used to determine any frequency offset between the transmitter and the receiver.[1] Pressing a switch on the printer records the current CRT screen display on paper.

All of the analog recorded signals as well as all digital recorded signals were processed using this system. The results chosen for this report (Figs. 11-14) are all from playback of digital recorded demodulates (lower left line in Fig. 7), except the clipper-processed ones, since we were not sure of the reliability of the analog recorded 7800 Hz sample clock signal. For the digital signals, the demodulates were formed during the field tests, and were recorded on the digital tape. The effect of averaging over 1, 4, 16 or 64 times was investigated by running the same digital cartridge repeatedly with different processing commands.[2]

---

[1]This feature was added to the program after the field test. The current program can also print out an estimated output SNR for each trace; this was not available during the data reduction for this contract.

[2]The data processing with clipping used the analog tape to generate a digital tape as shown in Fig. 9.

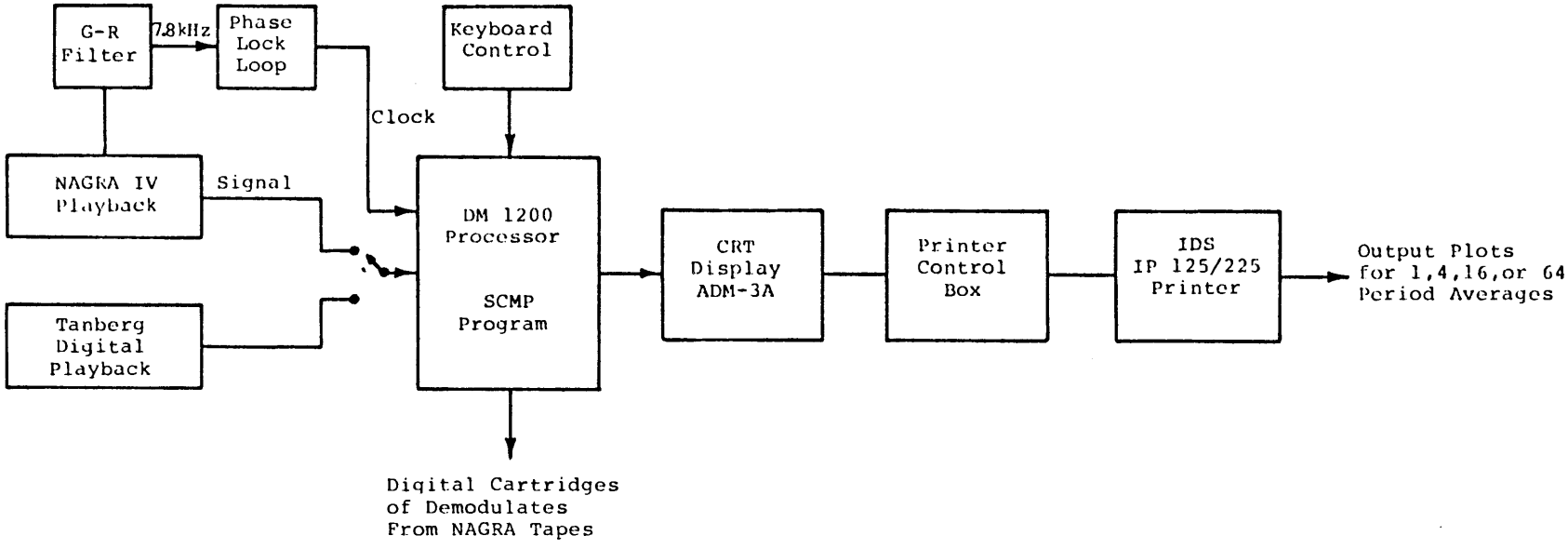

Figure 7. Data Processing Schematic for Output Time Axis Displays

Since the SCMP program was intended only for checking the data during the field test, there is no provision for converting the output to printed tables, or for recording it for further statistical analysis.

The second digital processing program was used to print out tables of numerical values. This program, shown in Fig. 8, is an updated version of the program used in our previous work. It differs mainly in that the matched filtering was always done before averaging over additional periods. Also, the data was recorded on 9-track reel-to-reel digital tape between processing steps. The demodulating and matched filter operations were done by the DM1200 using first the MTDEMOD and then the MTXC programs. The processed signal was recorded on the 9-track tape between the two steps. The matched filter output was again recorded on 9-track tape. Further averaging over a complete sequence bit, and averaging over 1, 4, 16 and 64 periods was done at The University of Michigan Computing Center on the AMDAHL computer using a PROG M5 program. This processing is essentially the same as that used and described in our previous work, Ref. 2, except that this time the matched filter operation was done by a second pass through the DM1200 computer using the MTXC program instead of using the AMDAHL. We did not run the output pulse displays on the AMDAHL because more completely labeled displays were already available from the SCMP program.

The digital demodulates recorded during the field tests are an alternate source of demodulates which replace the MTDEMOD program (see dotted line, Fig. 5c). The numerical results quoted here are all from the digital tapes. The 7800 Hz sample clock was less reliable on the analog tapes.

This program is much more flexible than the SCMP program, particularly since averaging operations are performed using Fortran programs running on the AMDAHL. However, the present AMDAHL programs, from PROG M1 through PROG M5, were all designed for displaying only the most recent 4 output pulses from each of the averaging procedures: x1, x4, x16, x64. This is convenient for an operator display, but makes it difficult to compare the effect of different averaging times for signals obtained in fluctuating background noise levels. For example, a stray noise source may have been present during most of the time that the 16 period and 64 period averages were formed, but turned off for part of the x4 and all of the last 4 x1 pulses. Some of the x4 and all 4 of the last x1 pulses may then appear to have a much better SNR than expected from the noise observed in the longer averages. This is desirable for the operator display. However, with only 4 pulses available for each increment of averaging, the numerical output for real mine data, even when all the numbers are averaged, is too variable to be very useful for statistical analysis. The graphical displays from the SCMP program are more useful for comparing different averages than the numbers from the PROG M5 program.

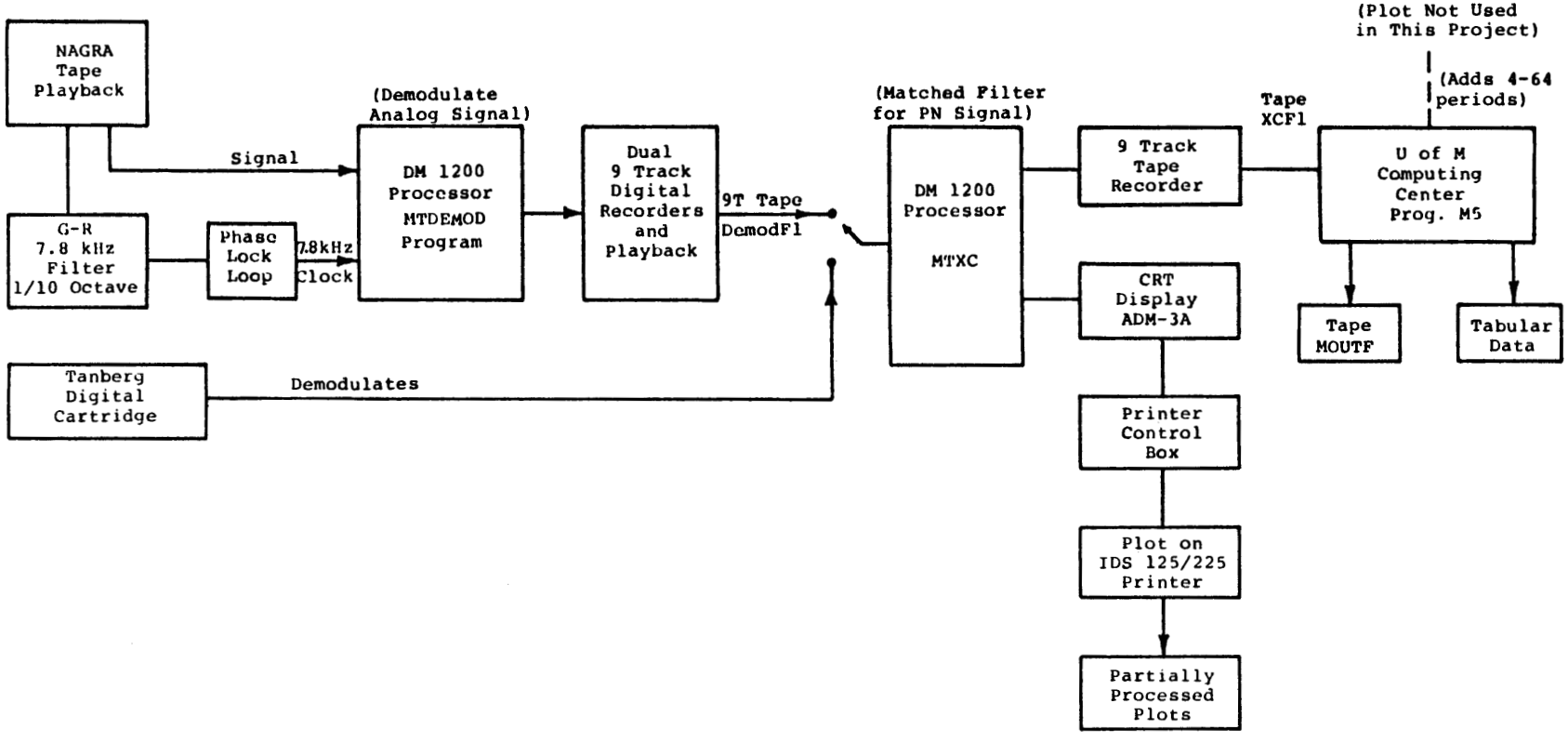

Figure 8. Data Processing Schematic for Output Printouts (See Appendix A)

The tapes used on the NAGRA tape recorder for Tests A and C were of poor quality and had many dropouts on the time reference track. We constructed a phase lock loop to track through these. In general it was successful, but we have no assurance that the time track is free of errors.

5.1 Off-Line MTXC Processing Arrangement

Figure 7 shows the sequence of steps used in the off-line signal processing of both the analog tapes, and digital-cartridge demodulate-tapes. Analog tapes are digitized and demodulated in real-time by the DM1200 using the MTDEMOD program. The output is stored on tape DEMODF1. The digital cartridge tapes were those produced by the SCMP program. The MTXC program performs the first step (sequence removal) in the matched filter processing for both types of recordings off-line and records the 4 chips for each signal bit on digital tape XCF1. At the U-M Computing Center, the 4 complex chips are combined for the single period output. The 4, 16 and 64 period averages are formed on a sliding window basis. The MTXC output is also plotted on CRT and printer, but this is before the 4 chips are combined.

5.2. Special Processing for Displays

In order to avoid preparing elaborate display programs for the off-line processing (above), we again exploited the DM1200 in the fashion shown in Fig. 8, for the purpose of achieving display output. The SCMP program generates processed signal displays like those generated at the Lake Lynn Laboratory during the field tests. The algorithm used for the matched filter is somewhat different from that used in MTXC. Also, the averaging over many periods is not done on a continuous sliding window basis, and therefore, the effect of normalizing the peak amplitude is slightly different. (It appears to us that this resulted in a more stable background noise level with the SCMP program). The displays of the test results (See Sec. 7) in this report are from this SCMP processing. A disadvantage is that, at present, the SCMP program does not generate a 9-track digital tape suitable for sliding window processing and numerical tabulation at the U-M Computing Center. We therefore, have no numerical data for comparing the two algorithms. Direct comparisons of the CRT or printer displays are not possible because the 4 complex chips are not combined in the MTXC process until the PROG M5 at the computing center.

5.3. Special Clipper Signal Processing

On Wednesday, more than one noise pulse occurred in most sequences, but the pulse amplitudes were comparable to the background noise. In contrast, the noise pulses on Thursday were both more numerous and much larger in amplitude. In addition to the isolated short noise pulses, there were bursts of periodic noise pulses, where, for many power line cycles, a large noise spike occurs in every cycle. The position of the spike shifts

slowly in phase from cycle to cycle during a burst. The largest bursts occurred regularly every 45 seconds during the Thursday test. Each large burst was followed by a smaller but longer burst of spikes 6 seconds later (Fig. 10). These bursts were present through all of the Thursday tests until the last few moments of the last test. Then, their source apparently was suddenly turned off.

Using the analog recordings, we did improve the Thursday results by subjecting the output of the input filter to a clipper. The pulse compression properties of the PN signal can be very effective in suppressing such noise pulses in a system designed for such conditions. (1) The signal duration should be such that only one (or a few pulses) is likely to occur in any one signal period. (2) Pulses much larger than the background noise should be clipped near the background noise level in a clipper with a bandwidth as wide as the noise pulses ahead of any narrow band filters. (3) A number of signal periods should be combined for reliable signal detection since some signal pulses may be reduced in amplitude by a long noise pulse or multiple pulses occurring in the same signal period.

Since all our PN test data was recorded with the 1/10 octave filter at the front end, the second condition was not met. Nevertheless, a very significant improvement was obtained by clipping the NAGRA output near the peaks of the background noise level using the arrangement of Fig. 9. Under the conditions of Tests Q, P, and E, the signal has a constant amplitude more than 40 dB below the background noise amplitude shown above. Clipping, therefore, has no effect unless an atmospheric noise burst is present. Then, the signal is largely suppressed during those times that the clipping levels are exceeded by the atmospheric burst. The signal segments that survive, however, still add coherently to form a (distorted) signal peak.

6. Input SNR Aspects

Input signal-to-noise ratio (SNR_i) is a suitable independent parameter for specifying the performance of a "detection" system, since: 1) the integration-time, and hence, signal energy, are variable due to the parallel processing; and 2) we wish to compare the performance to that of the present system.

6.1. Noise Types

Our original system design exploited the simplifying assumption that, if the major signal energy is contained between the relevant harmonics of the 60 Hz power system, the relevant background can be assumed to be stationary Gaussian noise. Also, the prior-effort laboratory demonstration tested the system in white Gaussian noise. It is known classically that, in Gaussian noise, with unknown signal phase (due to unknown onset and

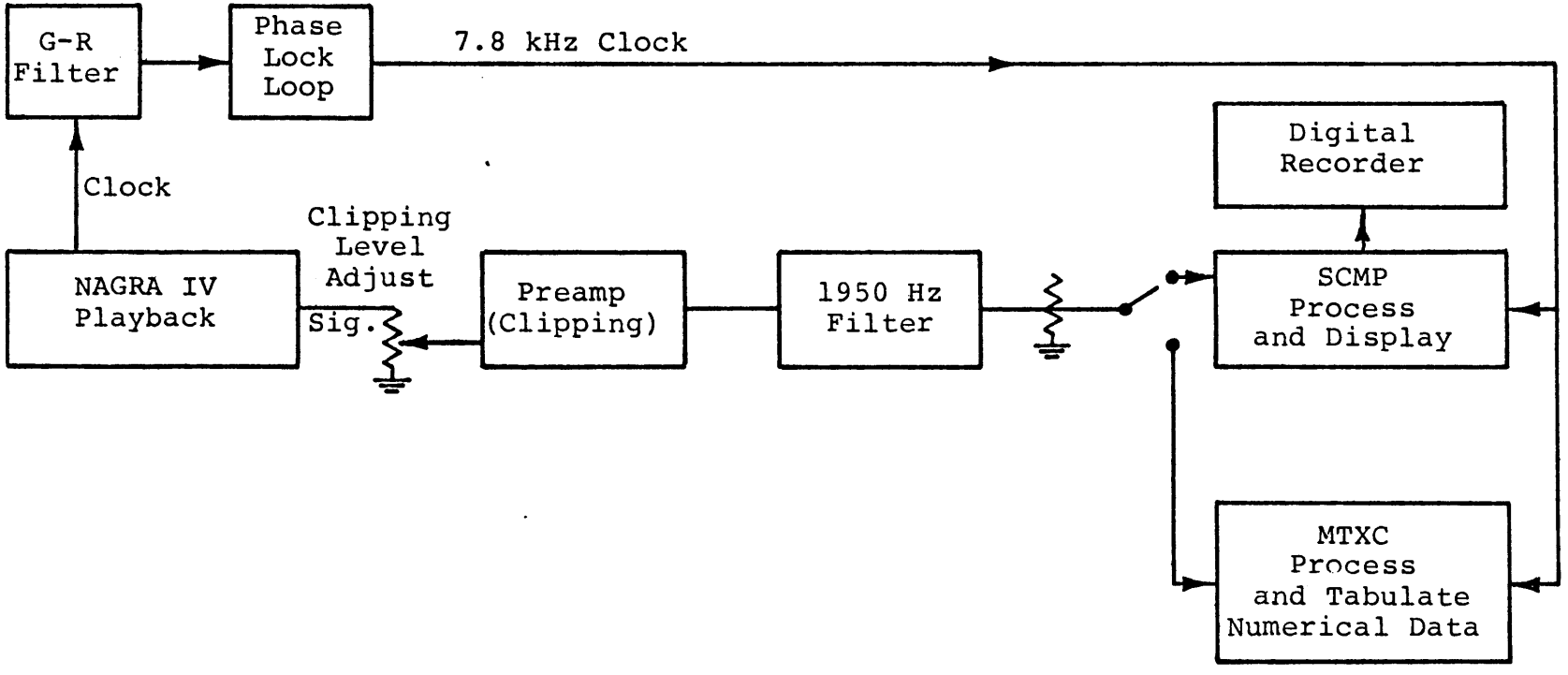

Figure 9. Block Diagram Used When Clipper Was Used in Data Processing

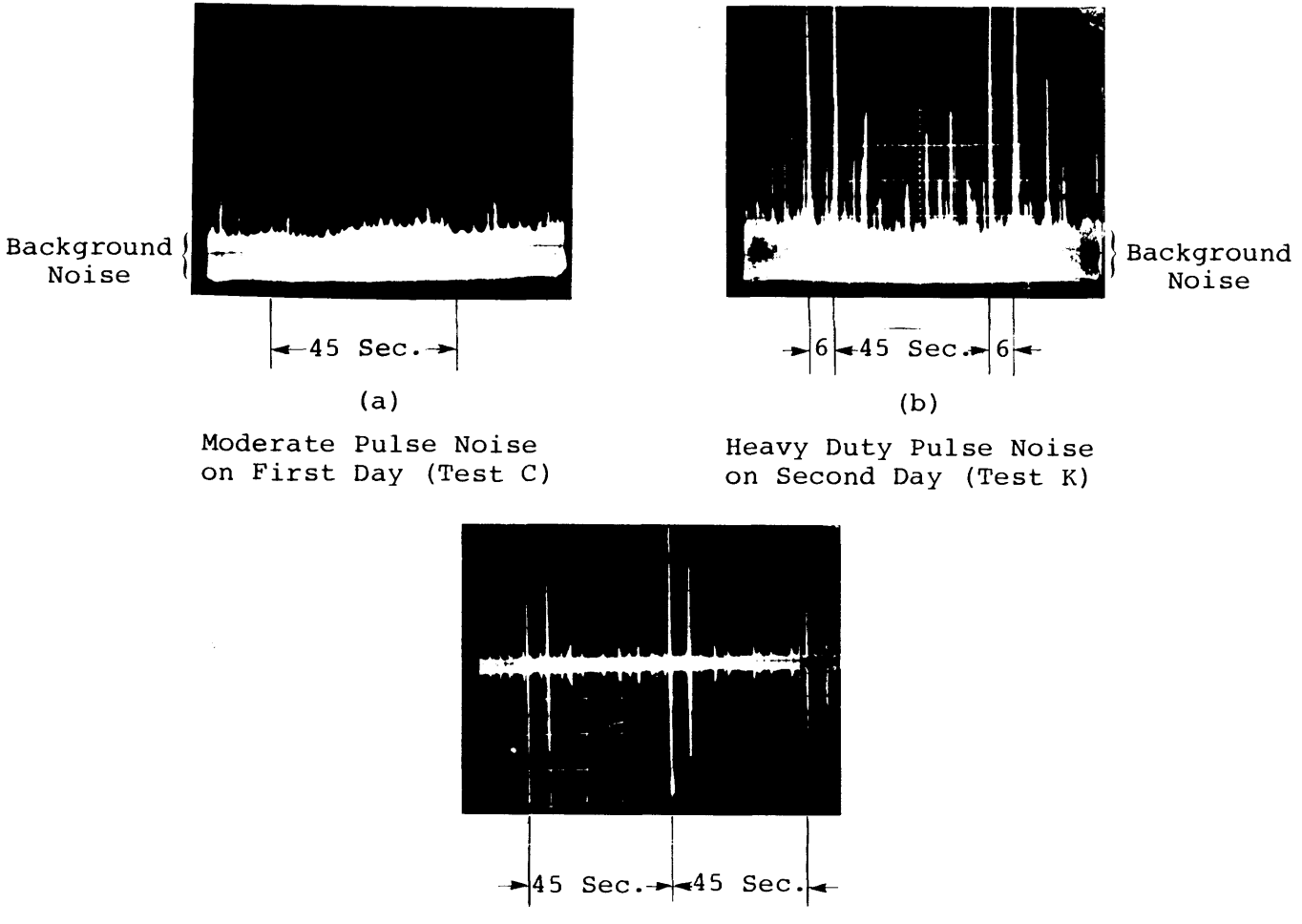

Figure 10. Noise Samples on First and Second Test Days

propagation delay), the optimum signal processor is a matched filter, as implemented by our signal processing receiver.

Both in preparing for and conducting the field tests, the signal was received using the Bureau of Mines supplied loop antenna. Both occasions provided us with experience of the effects of a (possible) combination of Gaussian noise, harmonic noise, and impulse noise.

The harmonic noise appears to stem from periodic transients in the power distribution line voltage. The important feature of this noise is that it is periodic.

The impulse noise may be due to either power line switching transients or atmospheric noise, usually from distant or local thunderstorms, that reach the antenna. If thunderstorms are within a few hundred miles, the noise becomes essentially non-stationary: heavy voltage surges are sporadically imposed on top of the normally varying background noise. Hence, when atmospheric noise is not present, the background noise is relatively well-behaved and coarsely measurable; with strong atmospheric noise, measurements are quite difficult.

For the test series described here, on Thursday we encountered an unusually large impulse noise from an unexplained source. The large impulses occurred every 45 seconds, and the major pulse was always followed by a smaller pulse 6 seconds later.

6.2. Input SNR Estimation

In usual communication operations, one uses the IF bandwidth to define and measure the input noise to a communications receiver. In the test arrangement here, no specific filter served as an IF-equivalent. Rather, the signal passed through a 1/10 octave filter, and the matched filter signal processing itself effectively filters the signal having a "main lobe" bandwidth. This was deemed superior to actually using a 30 Hz bandwidth filter centered at 1950 Hz in the front end. In effect, the signal processing receiver implements a filter corresponding to a bandwidth of approximately the reciprocal of the integrating time.

The result is that the input SNR can be measured only coarsely both because: 1) the actual noise is constantly varying; and 2) the noise bandwidth which gives the most appropriate measure here is relatively arbitrary. For this reason, three separate methods were used to estimate the SNR.

As noted, both the PN system and the present pulse system are designed to operate in one of the minimum noise regions between the harmonics of 60 Hz. The input SNR must be measured in the same minimum and with the same bandwidth as the system for a meaningful measurement. For both pulse and PN receivers, the

input bandwidth is usually taken to be the width of the main lobe of the $(\frac{\sin x}{x})^2$ signal power spectrum. These bandwidths are 20 Hz for the pulse system and 30 Hz for the PN system. As a compromise in the first estimation method, the signal and the noise were each measured in a filter with a nominal 22 Hz bandwidth tuned to a center frequency of 1950 Hz. A small correction was applied to estimate the noise in 20 Hz and 30 Hz-wide bands.

The noise power in this bandwidth was measured with true RMS reading voltmeters. Since we were interested both in the types of noise present and an estimate of the residual background noise after peak clipping, the noise power from the RMS voltmeter output, taken from the analog tape, was recorded on a stripchart recorder or storage oscilloscope screen for each of the tests (Fig. 10). These results, for each of the data tests, appear on the left-most column of the SNR estimates of Table 1.

A second estimate was based on a procedure suggested by the Bureau of Mines (S. Shope). During prior and independent measurements at the same field-test site, and using the same transmitting antenna, the Bureau of Mines (Ref. 5) measured the constant "Q" in the equation:

$$H_Z = \frac{INA}{2\pi d^3} Q \qquad (3)$$

where:

I = antenna RMS current

N = number of turns of antenna

A = area of antenna loop

d = length of transmission path

Q = factor representing the signal loss due to the conducting half-space

At 1950 Hz, the Q was determined to be .409.

If we had some way to estimate the H_Z coming from the noise-only measurements, we could obtain a theoretically-predicted estimate of the surface SNR during any given integration period. The Bureau of Mines has a method for computing an H_Z from noise measurements (see Appendix B). For our purposes, we used a theoretical H_Z value (.074 A/m) based on a minimum noise experienced at a previous mine which was not operating (Ref. 6). In any event, it may be true that surface noise at a non-

operating mine may be coarsely consistent at different locations and at different times. The numbers shown in the middle SNR column of Table 1 resulted from this exercise. Note that both this theoretical predication and the previous 22 Hz measured SNR do not include the large impulse noise.

The third method of estimating input SNR consisted of examining the output peak behavior relative to the intervening noise-only behavior, which now includes the impulse noise. The output peak-pulse value is interpreted as $E_b+n_\emptyset$, and the intervening values are interpreted as $n_\emptyset$. Then, using the classical relation:

$$E_b/n_\emptyset = (S/N)_i \times TW = (S/N)_i \times (\text{sequence length}) \qquad (4)$$

and

$$\frac{E_b+n_\emptyset}{n_\emptyset} \approx E_b/n_\emptyset \text{ if } E_b >> n_\emptyset \qquad (5)$$

A hand-calculated method was used to perform this estimate. The right-most column of SNR numbers in Table 1 resulted from this calculation. Examples of the output for this estimate appear in Appendix A. Appendix C contains the actual signal levels and noise levels that were used in the SNR estimates.

The following comments are intended to document what we learned about the noise behavior during these tests. During calibrating tests M,(PN), and L,(pulse), which were taken prior to the data tests on Thursday, the transmitting antenna currents were high enough so that the received signal voltages in the 22 Hz filter band measurement could be measured directly. The unmodified Collins antenna output was connected directly to the NAGRA recorder input for these tests. On playback, the NAGRA output was fed to the 22 Hz bandwidth filter and the output measured with the true RMS voltmeters. The signal voltage at the Collins antenna was then calculated from the known NAGRA gain settings.

In calibration test J, taken during the same period, the same system was used (with higher NAGRA gain settings) to record the background noise level. The noise power read by the true RMS voltmeters was recorded on a stripchart recorder and on a storage oscilloscope screen. The background noise level was estimated from these displays. It was assmed, as in the left part of the table, that the large and very unpredictable noise pulses would be removed by peak clippers in an operational system.

Considering the crude nature of the theoretical predictions, the directly measured input SNR and the backward-calculated one

appear consistent with the theoretical predictions. Note that from the measured Collins antenna voltage at this high transmitter current, one could calculate the Collins voltage for each of the other Test transmitter currents. This could be used to calculate a set of input SNR for the Collins antenna and the background noise of Thursday.

This is essentially what was done for the PN tests listed at the right edge of the table. However, the background noise voltage was the noise voltage measured at the output of the modified resonant Collins antenna used with the PN receiver, and the signal voltage was obtained from the strongest signals received with the modified antenna (Tests K, O, A, and C). Again, the input SNR for each test appears compatible with that in the other sections of this chart. Again, we would expect all of the tests signals (with clipping) to be detectable.

We note that the SNR does not depend on either the antenna gains or the system calibration as long as the same system is used for both the signal measurements and the noise measurements. There is general agreement in these values. However, the actual voltages for our resonant antenna system are roughly 30 times those expected for the theoretical non-resonant antenna used in the predictions at the right of the table. This appears consistent with some simple measurements we have made on the resonant antenna, but we have no absolute calibration for the antenna which we could use, for example, to determine the ground conductivity from the measured antenna voltages. The voltages we obtained for the unmodified Collins antenna are also higher than those predicted for a non-resonant system. This also appears consistent with our experience. Before we tuned our antenna, it was self-resonant roughly 3 KHz above our operating frequency. These points would have to be checked if the PN system were to be used for ground conductivity measurements. Fortunately, they have no direct effect on the communication system SNR calculations.

7. Test Results

After processing the tapes, it was found that the maximum sensitivity for the processing-receiver occurred for 16-sequence-long integration (4.46 minutes), and not for the expected 64-sequence length (17.854 minutes). Using the high signal levels in Test A, we were able to show that this result was due to some drift between the transmitting oscillator and the receiving oscillator. We do not know the reason for this drift, but the result is that, for these field tests, the optimum results occur when one limits the integrating time to 4.46 minutes. This is probably the maximum tolerable delay time in an operational system; nevertheless, for purposes of demonstrating maximum signal processing capability, we did originally intend to coherently integrate up to 17.854 minutes.

For Test A, (Fig. 11a), and Test C (Fig. 11b), the signals are detectable with 1, 4, 16 or 64 sequence additions. Hence, the earliest alarm in this case would have occurred in 16.74 seconds. Figure 11a shows six samples of the receiver output time axis when the minimum integration time (16.74 seconds) is used. The input SNR is estimated to be 20.4 dB. As seen in Fig. 11a, the output time axis shows no off-pulse activity, which means that the output noise is lower than the smallest digital quantization interval. The significance of this is that the input SNR is much larger than required. The data reduction program computed the received phase angle (A) for the time position identified as the maximum (reference) position. In Fig. 11a, we see that the phase angle changed by 15^{o} in 1.4 minutes. This indicates a transmitter frequency error of 2.6 parts in 10^{7}. Also, as seen, the output noise is at the resolution limit of the display (or lower).

Figure 11b shows the results of Test C, where the input SNR is estimated to be 2.14 dB, with integration time still equal to the (minimum) 16.74 seconds. Hence, again the alarm would have occurred 16.74 seconds after transmitter turn-on. Again, the input SNR is sufficiently high so that off peak output "noise-only" values are below the quantization level of the processor.

Figure 12a shows a series of six output time axes, from Test Q, when the input SNR was estimated to be about -11.7 dB, which included the erratic thunderstorm impulses and the large periodic impulses. The integration time is now 4.46 minutes, the longest effective integration time for these field tests (recall, the 17.854 minute integraton was less effective because of frequency drift between oscillators). We used the off-line clipping arrangement of Fig. 9 to achieve the clean results of Fig. 12a. Figure 12b shows the same data, with same integration, but without use of clipping.

Figure 13 shows a series of 10 output time axes for Test P, where the input SNR (with impulse noise excluded) was estimated to be about -19.9 dB. The integration time was again 4.46 minutes and clipping was required. We estimate that, for alarm purposes, the SNR is still somewhat above threshold for reliable detection with negligible false alarms.

Figure 14 shows a series of 10 output time axes for Test E, where the input SNR (with impulse noise excluded) was estimated to be -30.8 dB. The integration time was 4.46 minutes, and clipping was required. We believe this test coarsely corresponds to threshold operation for a reliable alarm system.

8. Conclusion and Recommendations

The major conclusion is that the field test described herein definitely demonstrated in the field the viability and potential

Key for Figs. 11 - 14:

C = Number of sequence periods

MAX = Time slot where maximum signal occurred

REF = Time slot at which phase angle (A) was computed

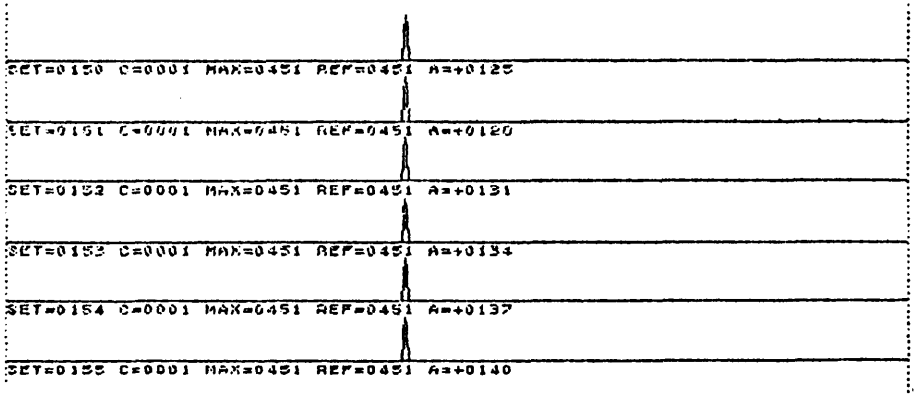

Transmitter Antenna Current (mA)	Integration Time (min.)	Estimated Input SNR (dB)	Estimated Output SNR (dB)
88.0	.279	20.4	50.0

(a) Data Test A

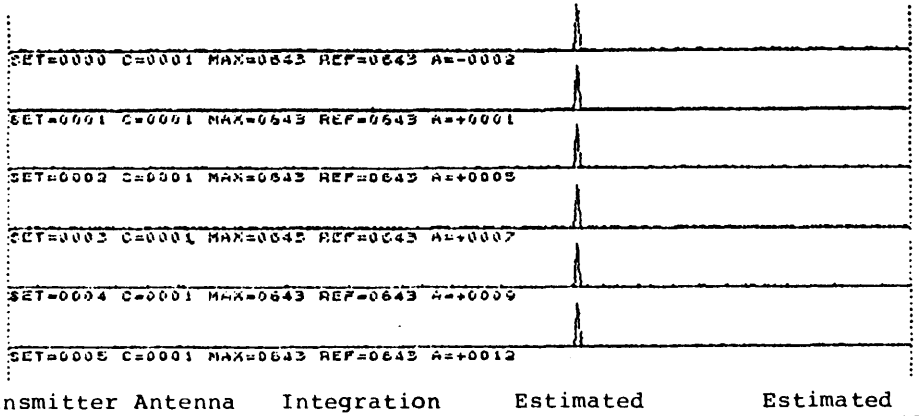

Transmitter Antenna Current (mA)	Integration Time (min.)	Estimated Input SNR (dB)	Estimated Output SNR (dB)
10.8	.279	1.9	21.0

(b) Data Test C

Figure 11. High SNR Output Time Axis Results

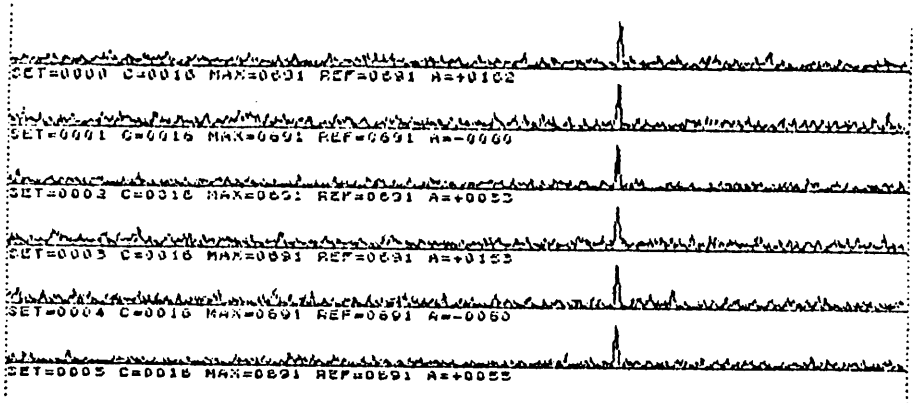

Transmitter Antenna Current (mA)	Integration Time (min.)	Estimated Input SNR (dB)	Estimated Output SNR (dB)
1.2	4.46	-14.2	21.8

(a) Clipping Used Prior to Matched Filter

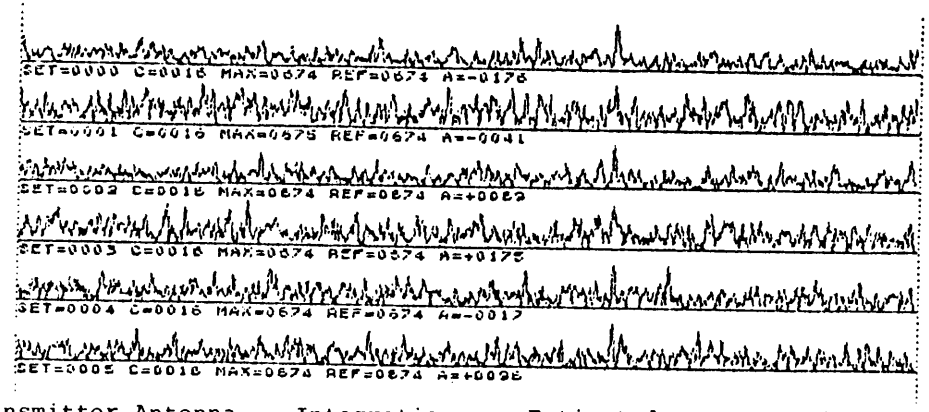

Transmitter Antenna Current (mA)	Integration Time (min.)	Estimated Input SNR (dB)	Estimated Output SNR (dB)
1.2	4.46	-14.2	11.4

(b) No Clipping Used in Processing

Figure 12. Intermediate SNR Time Axis Results (Test Q)

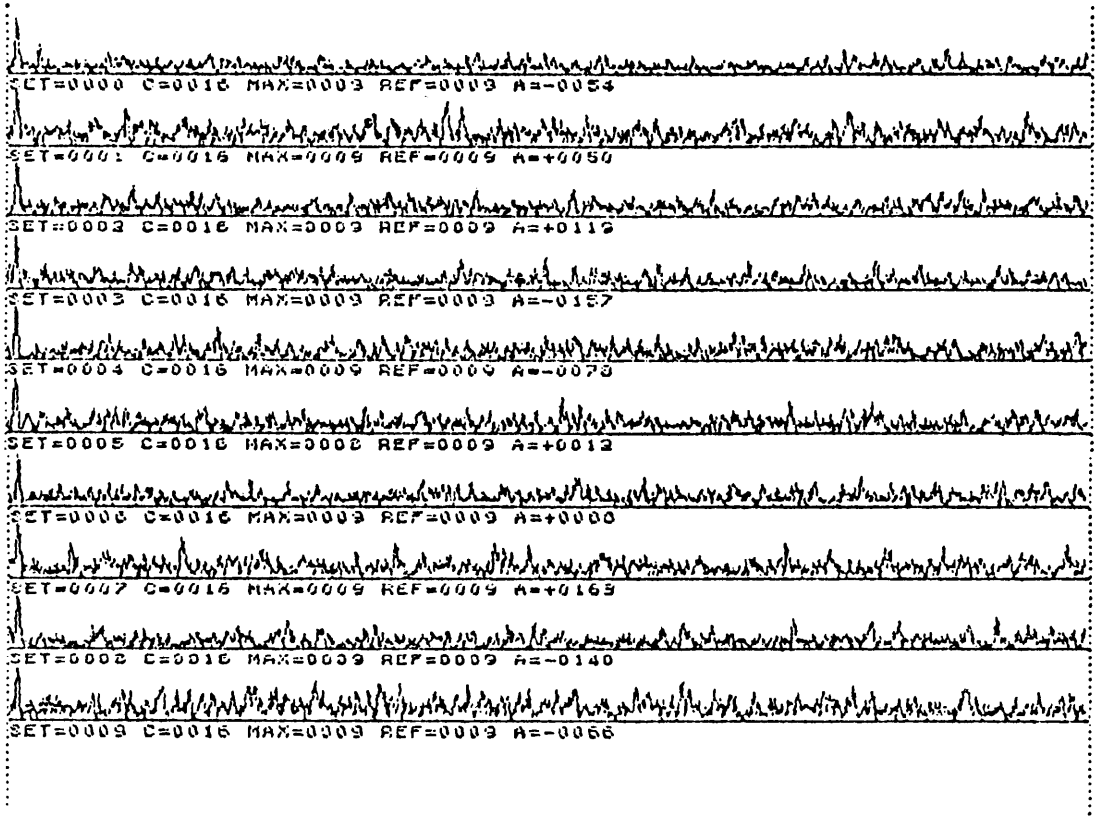

Transmitter Antenna Current (mA)	Integration Time (min.)	Estimated Input SNR (dB)	Estimated Output SNR (dB)
.68	4.46	-19.9	16.2

Figure 13. Low SNR Time Axis Results (Test P)

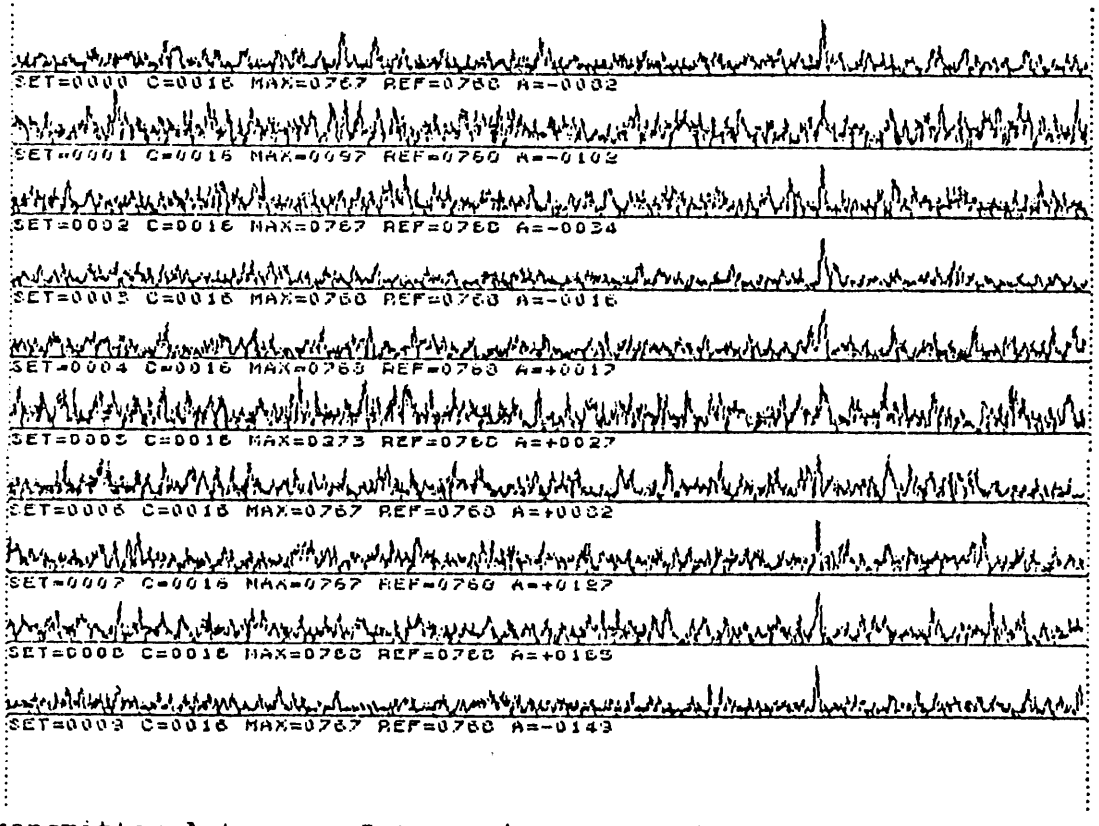

Transmitter Antenna Current (mA)	Integration Time (min.)	Estimated Input SNR (dB)	Estimated Output SNR (dB)
.25	4.46	-30.8	10.2

Figure 14. Threshold SNR Time Axis Results (TestE)

of the PN-signal plus coherent-integration technique that we are pursuing for the Bureau of Mines. We demonstrated, using integration times of 4.46 minutes, reliable operation at transmitter antenna currents of 0.25 mA, corresponding to about an input SNR of -30.8 dB.

The superiority of the PN signal was demonstrated during these field tests. One elementary but crucial aspect is the (relative) inherent detectability of the output "pulse" that results from matched-filtering a signal having an ideal (pulse) autocorrelation function. Another superiority of the PN signal-plus-stable clock results from the true-zero that occurs in the power spectral density at harmonics of the 60 Hz power system. The true zero apparently is reliable and stable because the large power-distribution system has a stable and well-controlled frequency. The stable oscillator used in our system, for coherent integration, in combination with the stable power-frequency, permits a suppression of harmonics which is difficult to match with steep-sloped filters.

Still another advantage of the PN signal here is its compatibility with extending the alarm-function discussed thus far to ensuing uplink communications. The pulse-output is sensibly compatible with a high M-ary pulse-position modulation. The achievable uplink data rate is proportional to $\log_2 M$ and inversely proportional to the total integration time required. This is discussed further later when considering recommendations.

The attractiveness of parallel processing, which implements an adaptive-type processing, was demonstrated during these tests. In effect, the alarm occurs at the earliest time, commensurate with the input SNR. Operational design (say) would probably aim to have the alarm occur at the minimum time (say 17 seconds). Then, the longer signal-processing times simply guard those conditions under which some unexpected phenomenon results in a lower SNR. Although elementary in concept, this appears to be thoroughly sensible for providing a reliable alarm and communication system.

As usually occurs, the field tests here revealed certain improvements that are sensible and warranted. First, we now realize that operation will be improved by using a clipper ahead of any filtering, which is adjusted to somewhat-above the "between 60 Hz pulses" level of the ongoing time axis. Such clipping will also do the best job possible of reducing the effect of atmospheric pulse noise. We would have experienced somewhat improved results from this field test if such a clipper had been used.

Another improvement would have been available if the frequencies had not drifted somewhat over the maximum planned interval of 17.84 minutes. Although we could establish, by detailed diagnostic examination of the data during the high SNR

tests, that the drift occurred, we do not know the cause. This aspect will warrant further attention in moving toward an operational system.

It is the authors' opinion that one significant application of the new system lies in using fixed-point, round-the-clock receiving sites to replace the initial detection now done by heliocopter-search followed by walking over the indicated area. Another significant application lies in using a localized null-seeking strategy to position-locate the transmitter.

Having now demonstrated the feasibility of an ultra-reliable signalling system, it is recommended that the system be refined and an implementation strategy be developed. Suggested refinements include:

a) Design and develop a surface "base station," that efficiently accomplishes the signal processing.

b) Investigate the possibility of uplink voice, using some low-bit-rate voice digitization, plus an efficient digital modulation.

c) Investigate position-location improvements and techniques that are offered with this signalling approach.

The implementation strategy should include consideration of general communication or measurement opportunities that are opened up by this system.

APPENDIX A

A Sample of the Printed Data Output of the PN Processor

Ervin Holland-Moritz

All of the analog recorded PN test data as well as the digital recorded PN data was processed and printed out in tabular form for detailed analysis. Including clipping tests, there are more than 25 sets of such printed tables, each consisting of more than 130 pages with 8 columns of data per page. Part of a sample page from the Test A output is shown in Table A-1. This sample is from the digital recording and was processed with no clipping or low frequency noise rejection.

The index column (1) on the left represents increasing time from start of processing in intervals of 8.2 milliseconds. In each time interval a new processed output is computed from the demodulates and printed in the following column. If any signal pulses are present, they will be separated by 2040 in the index number count, but the signal may start at any index number.

Columns (2) and (3) are processed outputs with coherent integration over only one PN sequence period. Column (2) consists alternately of the processed inphase demodulates and the processed quadrature demodulates. There are 4 pairs of demodulates per PN signal chip. Prior to index #901 and after #910, numbers represent alternately the inphase and quadrature noise voltages. In between, the voltages are a combination of noise and signal. The signal peak occurs at index #903. If the SNR is adequate, the received signal phase can be determined from the magnitudes of the adjacent inphase and quadrature voltages. Note that there are still 4 processed demodulates per signal pulse at this point. In the final processing, a coherent sliding window average over 4 pairs of demodulates is taken.

The processed output from column (2) is printed in column (3). The inphase processed demodulates are combined in a sliding window sum over 4 and the window output is squared. The quadrature demodulates are similarly combined and squared. The number printed in column (3) is the sum of the squares of the inphase and quadrature components. Note that the index number and sliding windows then shift by one demodulate so that each processed demodulate is used twice, once with its preceding quadrature component and once with its following quadrature component. Since these output numbers are based on samples taken at fixed time intervals, they can be interpreted either as (signal+noise) power or (signal+noise) energy. In particular, the peak number is the energy of the PN signal (with noise) after coherent integration over one sequence period.

Similarly, column (4) consists of processed demodulates

TABLE A-1. One Sample Page (of 140) from Test A: Digital Recording; No Clipping or Low Frequency Rejection

(1) Time Index	(2) 1X Demodulates	(3) 1X Output Power	(4) 4X Demodulates	(5) 4X Output Power	(6) 16X Demodulates	(7) 16X Output Power	(8) 64X Demodulates	(9) 64X Output Power	
887	23681	5392.0	2481	2544.1	-8929	10.6	-2250	30.0	
888	11853	5961.3	12202	2913.5	-6828	18.0	180	31.5	
889	-13935	3422.1	3813	2341.7	6788	16.9	2651	6.6	
890	1669	3157.8	-15916	1183.1	7592	56.9	-981	8.7	
891	20376	3959.9	5776	1196.4	-8654	215.5	-2293	3.9	
892	1617	4337.4	13849	2575.3	-5472	217.2	229	16.0	
893	-14312	3250.0	1919	2604.5	9949	174.4	2071	17.9	
894	1680	2978106.0	-17798	3455403.0	5291	7944.8	-1152	1715.4	
895	25570	3736862.0	3744	3726018.0	-9290	3551884.0	-2005	262510.1	
896	415	30822112.0	18622	32356960.0	-6923	3799034.0	1211	261037.6	
897	-14698	36411312.0	-633	35367680.0	10330	33904720.0	2850	2639746.0	
898	6736	92700096.0	-16368	94898256.0	3092	34520816.0	-331	2639207.0	
899	21456	103507344.0	10928	101272656.0	-8618	95879120.0	-1651	7585451.0	
900	-8181	188659248.0	17950	189772832.0	-4898	96833248.0	708X	7586275.0	
901	-578048	205107936.0	-601861	199592256.0	35554	189911680.0	-12284●	15106882.0	
Signal → 902	-274426	212018864.0	144317	202920912.0	604049	190696928.0	159904X	15127662.0	
903	-1162589	210086160.0	-1199699	205453184.0	122414	194626352.0	3730●	15932829.0	← Signal Peak
904	-520870	125203408.0	426935	116519472.0	1232144	193467632.0	353451X	15989422.0	
905	-1219393	109953056.0	-1236196	106141152.0	145789	101623264.0	10667●	8423239.0	
906	-506302	50879072.0	393437	46163920.0	1251043	100780960.0	356882X	8416314.0	
907	-1181275	40221824.0	-1206264	39030800.0	123468	37214352.0	6978●	3134778.0	
908	-531538	10125670.0	430848	8424583.0	1249658	36734704.0	358830X	3130332.0	
909	-660663	1938501.0	-640897	4562393.0	119258	4560238.0	25109●	414078.9	
910	-220930	578559.6	232273	634409.1	649117	4430643.0	194610X	407282.2	
911	3027	2171.8	9077	1772.3	-7498	2278.9	-91	293.1	
912	-22668	1.9	21830	2633.4	15171	2117.4	6468	294.0	
913	-17383	229.3	-20268	1656.5	11641	84.0	1585	56.9	
914	15955	814.0	-14422	1805.7	-705	104.2	-1025	47.1	
915	14556	957.3	25311	2072.6	-9474	59.5	-468	37.2	
916	-12438	943.9	12093	3849.5	2033	4.0	1751	51.3	
917	-14934	635.9	-21246	3323.9	9779	64.5	813	68.9	
918	19444	3718.4	-8256	3718.8	-2073	109.0	-2102	41.6	
919	17432	3722.9	27903	4963.8	-10041	52.6	-67	29.1	

Time from start of processing 8.2 millisec intervals	1X	4X	16X	64X
	$S=210x10^6$	$S=205.4x10^6$	$S=194.6x10^6$	$S=15.1x10^6$
	$N_{AV}=3319$	$N_{AV}=1709$	$N_{AV}=354.1$	$N_{AV}=57.4$
	S/N=623	$S/N=1.71x10^3$	$S/N=549.6x10^6$	$S/N=279.5x10^3$
	S/N=40.6dB	S/N=50.8dB	S/N=57.4dB	S/N=54.45dB

after coherent integration over 4 PN sequence periods. Each demodulate in this column is obtained from the average of 4 corresponding demodulates from 4 consecutive pulses in the column (2) data. Column (5) is the processed output after coherent integration over 4 PN sequence periods. It is obtained from column (4) by the same sliding window and squaring process described above for column (3).

Column (7) is the output after integration over 16 periods, while column (9) is the output after integration of 64 periods. In each case, the new processed demodulates are obtained by averaging the corresponding processed demodulates from 4 PN sequence periods from shorter integration time.

Because the new demodulates are obtained as an average, the ideal pulse outputs for a noise-free system with ideal integration of a constant signal should remain the same with increasing integration time. If the noise is uncorrelated with the signal (for example, in Gaussian noise), then the average noise power should decrease by 6 dB in going from one integration time to the next longer time. The detailed printed data can be used to determine if the system, operating in real mine noise, is performing as designed, and for finding improved processing algorithms for increasing the reliability of signal detection. However, this output is much too detailed for display to an operator in real time. Graphical pulse displays, obtained either by plotting these numerical tables (or obtained more directly from the SCMP processing sequence), are more useful in evaluating performance under operational conditions.

Note that in the present numerical processing, only the data for the most recent 4 pulses for each level of integration is saved in the computer arrays. The earlier data was used in calculating the longer term averages, but at a later time cannot be displayed separately without rereading the MTXC data tape. Since there are at least 128 PN pulse sequences in a single test, printing a complete list of all the data pulses in this detailed manner is impractical, especially in an operational system. On the other hand, it is quite practical to display 128 consecutive pulses on a graphical printer output.

The numbers printed at the bottom of Table A-1 are the computed signal powers and the average of the noise power samples for the particular pulses shown. Because the times of integration increase towards the right, the longer integration times may include large noise pulses which may, or may not have been present in the shorter data periods displayed towards the left.

We see that the coherent signal integration is quite good up to integration over 16 periods. Then the drift in transmitter frequency caused a significant loss in signal power. The average noise power varies widely from pulse to pulse because of the noise statistics. In some cases, it decreases at more than the

expected 6 dB in going from one integration time to the next. In other cases, the decrease is less than 6 dB. Any consistent decrease of less than 6 dB indicates that there is some correlation between the existing noise and the signal (for example, 60 Hz harmonics in the signal band). In principle, such correlated noise can be removed by improved processing algorithms.

APPENDIX B

Comparison of the Pulsed System to the PN Method

Steven Shope
U. S. Bureau of Mines

An objective of the June field test was to evaluate the performance of the PN communication method as a trapped miner location technique. The performance of the existing pulsed location system has been well defined through earlier research efforts. A rough approximation of the PN system's performance can be made by field testing the two systems at the same site under similar noise conditions. It must be realized that this comparison serves only as a crude estimate and is by no means conclusive.

At the Lake Lynn test site, the 1950 Hz pulsed trapped miner transmitter was chosen as the reference device. The underground antenna configuration was the same for both transmitters (pulsed and PN). The signals on the surface were tape recorded for later analysis. The current in the underground antenna was calculated by measuring the voltage drop across a shunt resistance placed in series with the antenna loop. An averaging FFT was used to make this voltage measurement.

Analysis of the surface vertical magnetic field revealed the pulsed transmitter produced 37.27 dB (re:1 amp/m). The vertical magnetic noise field excluding 60 Hz harmonics was 4.60 dB (re:1 amp/m). The net SNR on the surface due to the pulsed transmitter was 32.67 dB. The underground magnetic moment was 105 Amp-m^2 (.526 amps flowing in a loop of area 200 m^2). For the sake of argument, say the minimum detectable SNR (for some probability of detection and false alarm rate) is 10.2 dB. Since the system is linear, the pulsed transmitter must produce at least $.396 \times 10^{-2}$ amps (.526 amps down by (32.67-10.2)dB) for the signal to be detected on the surface. In other words, $.396 \times 10^{-2}$ amps would produce the 10.2 dB minimum SNR on the surface.

In test "E" of the PN technique, 250 amps were flowing in the loop. On the surface, after detection and processing, the receiver produced a 10.2 SNR output. Thus, we have similar signals from both systems, yet the PN method required only 250 amps while the pulse system required $.396 \times 10^{-2}$ amps. The difference in the two systems is 44.0 dB. This figure may be roughly used as the performance improvement one obtains by using the PN technique.

APPENDIX C

Input SNR Estimates

Ervin Holland-Moritz

Table C-1 contains the detailed numbers from which the input noise estimates of Table 1 (in text) were obtained. In addition, the table contains an additional set of "expected" noise and signal values. The "expected" field strength and the resultant antenna voltages were calculated from the equations in Table C-1, using Q=.409 from previous Bureau of Mines measurements at this site. The voltage equation assumes a non-resonant antenna coil. Measurements on the antenna coils indicate that both coils actually are resonant and this increases the antenna output voltage. The Collins antenna is self-resonant at a frequency considerably higher than the signal frequency. The exact resonant frequency is determined by the input impedence of the measuring device and the cable capacitance. The U of M antenna was tuned to be resonant at the signal frequency.

The expected noise used was taken as the "minimum" noise experienced in prior noise tests (Westinghouse Final Report), which were used by Collins in their receiver antenna design. These noise voltages are measured by the resonant antenna coils in the same proportion as the signal voltages. The calculated signal to noise ratios, therefore, are not affected by antenna resonances.

The total received noise was much higher on the second day, but the increase was largely due to impulse noise. The noise levels shown in Table C-1 were obtained from measurements of chart recording or storage oscilloscope images where the noise pulses were ignored and the continuous background noise was measured. The noise measurements for the second day, therefore, correspond to the expected noise levels after clipping.

Calculated in this way, the calculated SNR's for the processed PN signal appear consistent with the visual appearance of the corresponding processed time axis displays.

TABLE C-1. RECEIVER INPUT SIGNAL AND NOISE CALCULATIONS

Day	Test	Antenna Current	[1]Hz μA/M	[2]Expected Antenna Signal Voltage	[5]Noise Voltage	Input S/N	Measured Collins Antenna [4]Signal Voltage	[6]Noise Voltage	Input S/N	Measured U of M Antenna Signal Voltage	[6]Noise Voltage	Input S/N	SNR Measured from Output Print-Outs (Includes Impulse Noise)
Th	M	0.957A	12.46	10.84μV	.064μV	44.6dB	109.0μV	[6]0.507μV	47.0dB				
Th	L	[4]0.53 A	[4]6.85	[3]13.33μV	.064μV	46.4dB	157.2μV	[6]0.507μV	50.9dB				
W	A	88.25MA	1.15	1.00μV	.064μV	23.8dB				28.9 μV	2.75μV	20.4 dB	23.46
W	C	10.75MA	0.135	.1224μV	.064μV	5.6dB				3.52μV	2.75μV	2.14dB	9.473
Th	Q	1.2MA	0.016	.01367μV	.064μV	-13.3dB				0.393μV	2.83μV	-11.7 dB	-24.27
Th	P	0.68MA	0.0087	.0077μV	.064μV	-18.4dB				0.223μV	2.92μV	-19.9 dB	-36.6
W&Th	E	0.25MA	0.0032	.0028μV	.064μV	-27.2dB				0.082μV	2.85μV	-30.8 dB	-42.627
		Mine Noise - AC Power for Receivers Turned Off											
		Expected "Mine Minimum"					Measured Collins Antenna			Measured U of M Antenna			
Th	K	--	.074		[5].064μV						[6]2.45μV		
Th	O	--	.074		[5].064μV						[6]2.5μV		
Th	J	--	.074		[5].064μV			[6]0.507μV					

1. Ref. A $H_z = \left[\frac{NAQ}{2\pi d^3}\right] \times I$ $A = 200\ M^2$, $Q = 0.409$, $d = 100$ M, $N = 1$

2. Ref. 6 $V = \left[8\pi^2 \times 10^{-7} \times A \times F \times N\right] \times H_z = .87 * H_z$ $A = 0.113\ M^2$, $f = 1950$ Hz, $N = 500$

3. RMS during 1/10 second pulse

4. RMS averaged over 1 second/pulse

5. Calculated from minimum mine noise $H_z = .074 \frac{\mu A}{M}$, Ref. 6

6. Steady noise component only, measured in 22 Hz filter bandwidth. Does not include impulse noise.

REFERENCES

1. M. P. Ristenbatt, "Post-Disaster Communication Design-Concept," Final Report for Contract No. G0177073, Cooley Electronics Laboratory, The University of Michigan, Ann Arbor, Michigan, February 1979.

2. M. P. Ristenbatt and E. K. Holland-Moritz, "Evaluation and Demonstration of a New Post-Disaster EM Communication Technique for Mines," Final Report for Contract No. J0199109, Cooley Electronics Laboratory, The University of Michigan, Ann Arbor, Michigan, 1981.

3. Simmons, "Development and Prototype Production of a Trapped Miner Signalling Transmitter/Transceiver," Contract No. J0395017, General Instrument, Government Systems Division, Hicksville, New York, June 1981.

4. Kurt Metzger, Jr., "Signal Processing Equipment and Techniques for Use in Measuring Ocean Acoustic Multipath Structures," Doctoral Dissertation, The University of Michigan, Ann Arbor, Michigan, 1983.

5. Steven Shope, "Lake Lynn Field Test Site Electrical Characterization," Memo to M. P. Ristenbatt, July 1983.

6. Rockwell International, Collins Commercial Telecommunications Division, "Waveform Generator-Package and Receiver," U.S. Department of the Interior, Bureau of Mines, Contract No. H0242010 Final Report, November 1976, pp. 20 and 41.